EcoMat

WILEY

EcoMat FUNCTIONAL MATERIALS FOR GREEN ENERGY AND ENVIRONMENT

REVIEW OPEN ACCESS

A Review of Photonics-Driven Thermal Management: Strategies for Efficient Energy Generation and Saving

Joo Hwan Ko[1,6] | Doeun Kim[1,2] | Se Yeon Kim[1] | Youn Ju Na[1] | Hyeon-Ho Jeong[1,2] | Young Min Song[1,3,4,5]

[1]School of Electrical Engineering and Computer Science, Gwangju Institute of Science and Technology, Gwangju, Republic of Korea | [2]GIST InnoCORE AI-Nano Convergence Initiative for Early Detection of Neurodegenerative Diseases, Gwangju Institute of Science and Technology, Gwangju, Republic of Korea | [3]Department of Semiconductor Engineering, Gwangju Institute of Science and Technology, Gwangju, Republic of Korea | [4]AI Graduate School, Gwangju Institute of Science and Technology, Korea Advanced Institute of Science and Technology, Gwangju, Republic of Korea | [5]School of Electrical Engineering, Korea Advanced Institute of Science and Technology, Daejeon, Republic of Korea | [6]Department of Mechanical Engineering, Massachusetts Institute of Technology, Cambridge, Massachusetts, United States

Correspondence: Hyeon-Ho Jeong (jeong323@gist.ac.kr) | Young Min Song (ymsong@kaist.ac.kr)

Received: 24 February 2025 | **Revised:** 24 May 2025 | **Accepted:** 8 July 2025

Funding: This work was supported by the GIST-MIT Research Collaboration through a grant funded by the GIST and National Research Foundation of Korea (NRF) funded by the Ministry of Science and ICT (RS-2025-16902996, 2021M3H4A1A04086357). This work is also supported by the Technology Innovation Program (RS-2024-00467230) funded by the Ministry of Trade Industry & Energy (MOTIE, Korea). J.H.K. acknowledges the support from the NRF (RS-2024-00345558). This work was also funded by InnoCORE-GIST program of the Ministry of Science and ICT.

Keywords: energy device | energy saving | photonics | photothermal effect | thermal radiation

ABSTRACT

Across a broad spectrum, photonics facilitates thermal management by manipulating electromagnetic waves in energy devices, enhancing energy production and efficiency. The light–matter interaction should be explored not only from the perspective of their individual heating/cooling functions but also for their mutual utilization. Here, we review recent advancements in thermal management strategies from a photonic structures viewpoint, presenting the comprehensive strategy that spans heating and cooling. We focus on strategically designed photonics, considering material properties that interact with the long-wave infrared spectrum at wavelengths from 8 to 13 μm, which are optimized for thermal emissions, and utilize the ultraviolet–visible–near infrared spectrum of the solar irradiance band for photothermal heating. Furthermore, exploring the potential for utilizing multiple wavelengths simultaneously forms the basis of a comprehensive photonics design strategy that leverages a broad spectrum of wavelength bands. This review evaluates the role of photonics in temperature control, thermoelectric generation, steam production, photocatalytic reactions, and radiative cooling, concluding with a discussion of the challenges and future directions in photonics for energy systems, highlighting the importance of a deep understanding of these interactions to maximize their potential.

1 | Introduction

In photonic designs for energy devices, the manipulation and confinement of light play crucial roles in enhancing energy generation and conservation [1–5]. The interplay between light and matter significantly improves the efficiency of heating and cooling applications, which are vital for boosting device performance and extending their lifespan [6]. This exploration highlights the role of photonic interactions within energy systems, emphasizing the manipulation of electromagnetic waves and their consequential impact on device functionality [7–8]. The profound capability of solar energy to swiftly meet global energy demands accentuates the importance of understanding electromagnetic interactions with Earth's atmospheric conditions [9–10]. Targeting

Joo Hwan Ko and Doeun Kim contributed equally to this work.

specific wavelength bands, particularly from ultraviolet (UV) to visible to near infrared (NIR) spectrum, unveils opportunities to optimize energy capture and utilization [11–12]. Additionally, a transparent window in the long-wave infrared (LWIR) of 8–13 μm within Earth's atmosphere presents a pathway for passive cooling [13–16]. This spectral region, characterized by minimal atmospheric radiative emissions and aligning with the peak thermal radiation of a black body at approximately 300 K as defined by Planck's law, enables efficient heat dissipation through radiative emission, providing a natural and energy-efficient cooling mechanism for terrestrial devices [17–19].

The adoption of integrated technologies that synergistically combine cooling and heating functionalities is crucial for advancing high-efficiency thermal management systems [20–21]. Rather than relying on isolated wavelength bands for specific thermal effects, cutting-edge photonic strategies seek to enhance overall performance by coordinating multiple light–matter interactions across the spectrum. The scope of photonic applications extends beyond the simple use of individual wavelength bands for heating and cooling [12, 22–27]. It involves the strategic manipulation of material properties and device architectures to enhance thermal management. For instance, Li et al. [28] enhanced the photothermal response by optimizing the thickness of a Bi_2Te_3 thin film on copper, which minimized heat loss from radiation and convection, thereby achieving a heating effect of 317°C under standard sunlight conditions. Meanwhile, Tang et al. [29] demonstrated a smart window that adaptively adjusts temperature using materials that alter their emission and visible-NIR transmission characteristics based on the ambient temperature. These advancements underscore the necessity for a comprehensive understanding of light–matter interactions across various electromagnetic wavelengths to design effective energy systems.

This review offers a comprehensive examination of thermal management systems considering a broad spectrum of wavelengths. The discussion commences with the introduction of optically tunable materials and their mechanisms, followed by categorized potential applications segmented by their purpose in utilizing electromagnetic waves. This includes photothermal absorption (UV, visible, NIR) and thermal radiation, along with LWIR applications. Each category is explored regarding heat management techniques and recent innovations in the field. This examination aims to delve into these interactions, exploring theoretical foundations and practical applications to pave the way for next-generation photonic energy devices that are efficient and adaptable to environmental and operational demands.

2 | Fundamentals of Photonic Platforms for Energy Devices

2.1 | Earth's Environmental Dynamics: Heating and Cooling Mechanisms

In this section, we briefly overview examples of the light–matter interactions facilitated by photonic platforms, focusing on their implications for energy production and conservation within Earth's environmental conditions. We examine instances where photonic technologies are deployed for both heating and cooling applications. Earth, situated within the habitable zone, achieves a delicate equilibrium between the heat from solar radiation and the cold of outer space, thus maintaining life-supporting temperatures [30]. Figure 1a provides a schematic depiction of sunlight traversing from the sun to Earth, triggering a photothermal effect. Significantly, although the energy Earth receives from the sun is just a minuscule fraction—one 2.2 billionth—of the sun's total radiative output, it still amounts to approximately 173,000 terawatts [31]. Remarkably, the solar energy reaching Earth in merely 1 h could meet the global energy demands for an entire year [32]. Utilizing this solar radiation as a primary energy source in thermal devices can greatly enhance both energy production and conservation, underscoring the pivotal role of photonic integration in advancing environmental management and sustainable development strategies [33–34]. In contrast, Figure 1b presents a scenario utilizing radiative cooling, a passive strategy that exploits the LWIR spectrum to effectively emit heat toward space, where the temperature is around 3 K [35–38]. This method leverages the vast coldness of outer space to dissipate heat, thereby facilitating thermal management by reducing temperatures on Earth [39–42]. By significantly reducing temperatures without relying on electricity, this method offers a viable and sustainable solution for thermal management across diverse sectors. Figure 1c illustrates sky transmission aligned with the AM 1.5 global solar spectrum, noting that solar irradiance mainly covers the UV–visible-NIR spectral range, whereas sky transmission is optimized between approximately 8 and 13 μm [43–45].

2.2 | Photonic Platforms to Regulate Thermal Energy

Figure 1d demonstrates how the photonic design can manipulate both the absorption of solar radiation and the emission of heat radiation into space, effectively managing the device's thermal characteristics. Moreover, heat exchange is influenced by the interactions between light and matter and external environmental factors [46]. The transfer of thermal energy between materials is governed by temperature gradients and manifests through three primary mechanisms: conduction [47–48], convection [49–51], and radiation [52–54]. Thermal conduction typically occurs within a material or between adjoining objects, as heat spontaneously moves from regions of higher temperature (the light absorber) to those of lower temperature (the heat transfer object) [55]. Thermal convection pertains to heat transfer prompted by fluid movement [56]. Thermal radiation transpires across all materials through electromagnetic waves, irrespective of any medium, as governed by the Stefan–Boltzmann law, where the emitted energy scales with the fourth power of the object's temperature [57]. An object emitting thermal radiation based on its temperature concurrently absorbs radiation from the environment, resulting in a net energy exchange between warmer and cooler entities [30]. Therefore, the strategic selection of photothermal materials and their environmental context is essential for targeted photothermal applications. Figure 1e,f elaborates on the diverse thermal and photonic strategies required for effective heating and cooling, highlighting the necessity for optical structures to integrate multiple elements to proficiently manage thermal properties intricately.

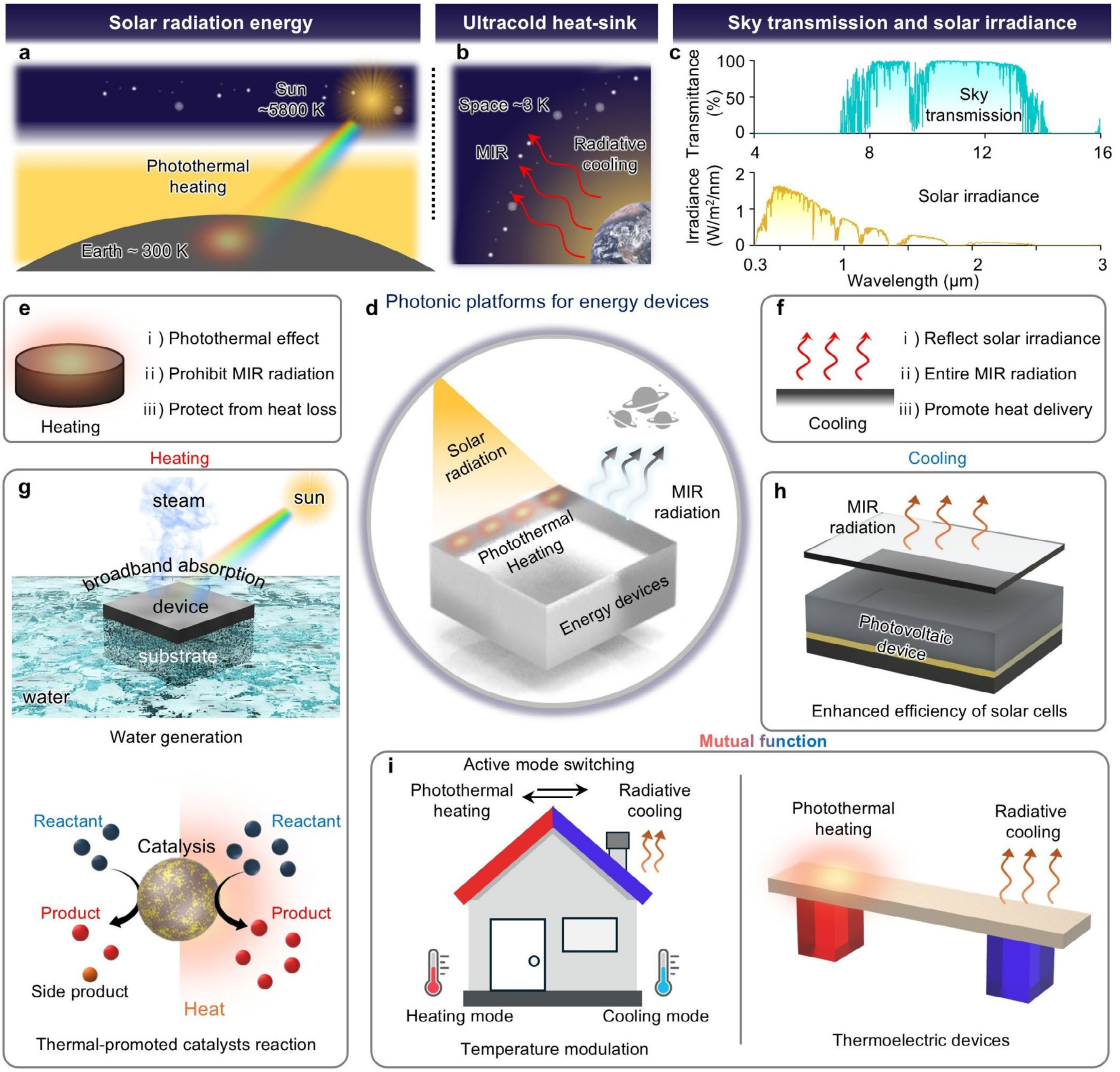

FIGURE 1 | Overview of earth environment and strategies of photonics-driven energy saving and generation. (a) Schematic illustrating the conversion of solar radiation to heat via the photothermal effect. (b) Schematic depicting the emission of thermal radiation from Earth to the ultracold temperatures of space. (c) Transmittance of the Earth's atmosphere (top) and solar irradiance (bottom). (d) Conceptual illustration of a photonic structure integrated onto energy devices, facilitating heating and cooling functions. (e, f) Representative strategies for heating (e) and cooling (f) in energy devices. (g) Thermal energy-assisted applications utilizing photothermal energy for steam generation (top) and photocatalytic reactions (bottom). (h) Integration of radiative cooling structures to enhance photovoltaic device efficiency. (i) Mutual function of heating and cooling for temperature modulation (left) and thermoelectric devices (right).

2.3 | Energy Devices Integrated With Photonics

This section explores the representative cases of photonics within energy devices, illustrating how advanced optical techniques are applied to enhance efficiency and functionality. For example, Figure 1g demonstrates a strategy that leverages solar energy absorption to generate high temperatures, which facilitates water desalination [58–60] or enhances the reactivity of catalysts [61–63]. This approach strategically maximizes light absorption to optimize thermal energy, while minimizing heat losses due to radiation and convection to maintain the highest possible temperature. Figure 1h presents an example of using radiative cooling to prevent performance degradation in solar cells caused by high temperatures, thereby achieving highly efficient photovoltaic (PV) devices [64–66]. Figure 1i shows how these two thermal management strategies can be mutually utilized to implement switchable temperature control systems and thermoelectric devices [67–70].

In addition to conventional heating and cooling devices, emerging photonic strategies have explored radiative warming and spectral engineering for infrared camouflage. Radiative warming leverages the infrared opacity of the atmosphere to retain thermal radiation near the surface, offering passive heating solutions particularly suitable for cold environments [71]. Radiative camouflage, by contrast, involves suppressing thermal emission in atmospheric transparency windows while selectively emitting in non-atmospheric bands, enabling reduced infrared visibility for thermal imaging applications [72–74]. These approaches expand the landscape of photonics-driven thermal management, with implications in building insulation, defense technologies, and intelligent thermal coatings.

3 | Photothermal Energy Conversion

To maximize platform efficiency through effective photothermal conversion, evaluating the device's light absorption and heat generation characteristics is crucial [75]. This requires considering physical models that describe light harvesting, light-to-heat conversion, transfer, and dissipation to achieve the desired cooling or heating performance. In this section, we present fundamental equations for photothermal conversion.

3.1 | Light Harvesting and Light-to-Heat Conversion

This review focuses on enhancing the performance of thermal management devices that utilize the solar spectrum as a light source. Absorptance, which quantifies the fraction of incident solar radiation captured by a material, is crucial in this context. It is defined as the fraction of an incident photon's energy absorbed by a material. The total solar absorptance of a material is determined by integrating its spectral absorption across the solar spectrum [76].

With the solar spectral irradiance distribution of the standard AM 1.5 solar spectrum at an incident angle θ, the total solar absorptance $A(\theta)$ of the device can be expressed as follows [77–78]:

$$A(\theta) = \frac{\int_{\lambda_{\min}}^{\lambda_{\max}} [1 - R(\theta,\lambda) - T(\theta,\lambda)]P(\theta,\lambda)\, d\lambda}{\int_{\lambda_{\min}}^{\lambda_{\max}} P(\lambda)\, d\lambda} \tag{1}$$

where $P(\lambda)$ represents the wavelength-dependent radiation power, and $\lambda_{\max}$ (~2.5 µm) and $\lambda_{\min}$ (~0.3 µm) define the solar spectral range of the incident light. $R(\theta,\lambda)$ and $T(\theta,\lambda)$ stand for the total reflectance and transmittance of the devices at the wavelength λ, respectively.

The photothermal effect is a fundamental phenomenon in light–matter interactions, where a material's temperature rises due to light harvesting. Light-to-heat conversion efficiency varies across materials, primarily due to differences in electronic structures and band gaps that determine their response to radiation. A detailed discussion of these mechanisms will be provided in the next section (Sections 4.1–4.3). Here, the focus is solely on the heat flux generated during the light-to-heat conversion process. Conversion efficiency is not determined by its ability to absorb light, but by how effectively it converts that absorbed light into thermal energy. This quantifies the proportion of absorbed energy that is transformed into heat rather than being lost through radiative emission. The photothermal conversion efficiency of devices, η, is expressed as follows [79–80]:

$$\eta = \frac{Q}{E} = \frac{cm\Delta T}{pst} \tag{2}$$

where Q is the generated thermal energy by the thermal management device, E denotes the total solar energy input. c and m correspond to the specific heat capacity and mass of the photothermal material of the device, respectively. ΔT indicates the temperature increase of the material. p refers to the power density of the light source, while s and t represent the radiation area and time, respectively. For solar heating applications, materials must exhibit high absorptance across the solar spectral range while minimizing reflectance and transmittance to maximize energy capture and conversion into heat (see Section 4) [81]. This ensures efficient photothermal performance, particularly for applications requiring rapid and effective heat generation. Conversely, cooling systems should be designed to minimize absorptance within the solar spectrum, thereby reducing parasitic heat gain and enhancing radiative cooling efficiency (see Section 2.1) [82]. Achieving an optimal balance between light absorption and heat dissipation is essential for tailoring photothermal materials to specific thermal management applications [68, 81]. Future advancements in material engineering, including nanostructured surfaces [83], thermochromic materials [70], and electrochromic material [84], could further improve light-harvesting efficiency and heat conversion performance.

3.2 | Heat Transfer

Once solar light is absorbed by a photothermal material of the devices, its photon energy undergoes conversion into thermal energy through a light-to-heat transformation process [75]. The generated heat is subsequently transferred to adjacent lower temperature materials or dissipated into the surrounding environment. Thus, heat transfer constitutes a crucial step in a photothermal conversion system. The thermal movement energy between materials occurs due to temperature gradients, which drive the process through three primary mechanisms: conduction, convection, and radiation.

Thermal conduction describes heat transfer within a solid or between adjacent materials in direct contact. In a photothermal system, heat spontaneously moves from a high-temperature region, such as a light-absorbing surface, to a cooler region, such as a heat transfer medium. This process follows Fourier's law and can be expressed as follows [77, 85]:

$$Q_{\text{cond}} = \frac{ks}{L}\left(T - T_{\text{dev}}\right) \tag{3}$$

where k is the thermal conductivity of the photothermal material, s is the surface area involved in heat transfer, L is the conduction length of the light absorber, and T_{dev} and T represent the steady-state temperatures of the heat transfer medium and the light absorber, respectively.

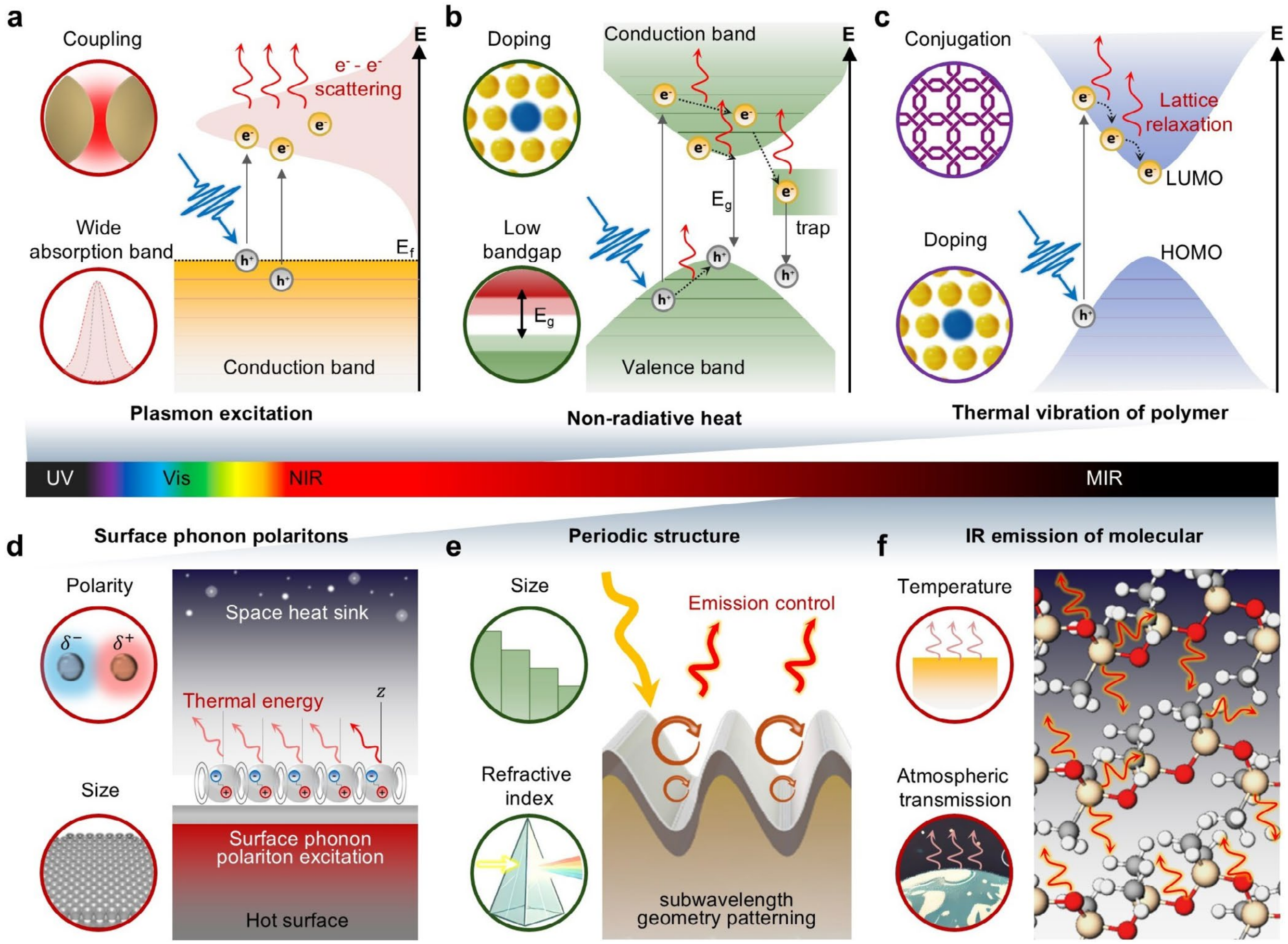

FIGURE 2 | Photothermal and radiative cooling mechanisms according to spectral absorption and emission ranges. Photothermal mechanism and enhancement strategy in (a) plasmonic local heating, (b) nonradiative heating of semiconductors, and (c) thermal vibration of polymer. Radiative cooling mechanism and enhancement strategy in (d) surface phonon polariton, (e) periodic structure of phonic devices, and (f) IR emission of molecular.

Thermal convection involves heat transfer through fluid movement, such as air and water. The heat energy transferred from the heat source to the fluid is described by [79–80]:

$$Q_{conv} = hs\left(T - T_{sur}\right) \tag{4}$$

where h is the heat transfer coefficient, which is the reciprocal of thermal resistance. The value of h is influenced by the fluid's physical properties and the thermohydraulic conditions of the system. T_{sur} is the surrounding fluid temperature.

Lastly, thermal radiation does not require a medium for heat transfer, unlike conduction and convection. This mechanism involves the emission of electromagnetic waves, where the emitted thermal radiation is proportional to the fourth power of the object's temperature, as described by the Stefan–Boltzmann law. When an object emits thermal radiation, it also absorbs radiation from its surroundings. The net thermal radiation exchange between a heated object and its cooler environment is given by [30, 86]:

$$Q_{rad} = \varepsilon\sigma s\left(T^4 - T_{env}^4\right) \tag{5}$$

where ε represents the emissivity, σ is the Stefan–Boltzmann constant, and T_{env} denotes the ambient temperature.

The efficiency of heat transfer is governed by both the intrinsic properties of the photothermal material and its surrounding environmental conditions. The three heat transfer mechanisms discussed above provide fundamental approaches to optimizing thermal management. Ultimately, designing appropriate photothermal device structures and optimizing their interaction with surrounding media are critical for achieving the desired thermal management performance in energy applications [87].

4 | Light–Matter Interactions for Heating and Cooling

Thermal management devices with photothermal heating and radiative cooling enable high efficiency of light–matter interaction by material composition and surface structure engineering (Figure 2) [30, 40, 43, 88–89]. For heating applications, maximizing light-to-heat conversion efficiency requires materials with high solar absorptivity [90]. This section explores the material properties of metals [91–93], semiconductors [94–95], and organic polymers [96–99] that facilitate heat generation through light–matter interactions. Additionally, radiative cooling is a passive cooling technique that dissipates heat by emitting MIR radiation [100], unlike conventional cooling methods that consume energy and release waste heat to the surroundings. We examine cooling strategies that promote heat dissipation [101], IR reflection with surface structure [30], and enhance IR emissivity of molecules across IR wavelengths [102].

Importantly, radiative cooling performance strongly depends on minimizing heat gain from solar radiation. Although MIR emission is critical for dissipating heat, effectively reflecting or scattering incoming solar radiation significantly contributes to the thermal capability. In this section, we specifically focus on material properties that facilitate such solar-band reflectivity or scattering. Various structural approaches enhancing solar reflection and scattering performance are comprehensively addressed in Section 5.

4.1 | Plasmonic Localized Heating in Metal

Metal nanoparticles exhibit strong light absorption and efficient light-to-heat conversion through localized surface plasmon resonance (LSPR) [103–104]. This phenomenon arises from the coherent oscillation and excitation of free electrons within the nanostructure upon light irradiation. Subsequently, hot electrons are generated as they interact with lower-energy electrons through inelastic Coulombic scattering (Figure 2a) [105]. This process occurs after lattice heating, which leads to phonon generation [106]. Enhancing the photothermal effect can be achieved using nanoparticle dimers [107–108], where plasmonic coupling concentrates the electric field in the gap [109], boosting heat generation. Alternatively, complex nanoparticles with asymmetric geometries or material composition enable broadband absorption, further enhancing photothermal efficiency [110–111]. These plasmonic structures have demonstrated solar absorptance above 0.98 and photothermal conversion efficiencies near 90% [110].

4.2 | Nonradiative Heating in Semiconductor

Nonradiative heating in semiconductors refers to the energy transfer between molecules without light emission, resulting in heat generation (Figure 2b) [112]. The absorption of semiconductors in the UV–visible region is governed by the generation of free carriers, which depends on the band gap [113]. When photons with energy greater than the band gap are absorbed, electron–hole pairs are generated. These excited carriers then relax to the band edge, releasing excess energy as heat through the thermalization process [77]. Compared to metals, semiconductors have lower free carrier concentrations, but this can be enhanced by doping or vacancies, improving light absorption and photothermal efficiency [77, 114]. These modifications increase nonradiative recombination, enhancing heat generation. Additionally, narrow band gap semiconductors further boost efficiency by absorbing most solar photons above the band gap.

4.3 | Thermal Vibration of Polymer

Certain organic polymers exhibit strong light absorption and efficient heat generation through lattice vibrations. While typical carbon bonds (C—C, C—O, and C—H) have large energy gaps between σ and σ^* orbitals that are difficult to excite, loosely bound π electrons can be easily promoted from π to π^* orbitals under low-energy irradiation [115–116]. π–π^* transitions can occur more readily under visible or NIR, enabling efficient light absorption with lower energy photons. When incident photon energy matches an electronic transition, π electrons are excited from the highest occupied molecular orbital (HOMO) to the lowest unoccupied molecular orbital (LUMO) (Figure 2c) [117]. After excitation, these electrons return to the ground state by transferring their energy into lattice vibrations (thermal vibrations) through vibration–electron coupling. This nonradiative relaxation process effectively converts the absorbed optical energy into heat. Additionally, conjugated and doped polymers reduce the HOMO–LUMO energy gap, facilitating easier π–π^* electronic transitions and improving overall efficiency in converting absorbed photons into heat [117–118].

4.4 | Heat Dissipation by Surface Phonon Polaritons

One mechanism involved in radiative cooling for MIR emission and parasitic heat reflection is surface phonon polaritons (SPhPs), which arise from resonant interactions between photons and the optical phonon modes associated with polar materials (Figure 2d) [101, 119]. Specifically, materials possessing polar bonds, such as Si—O (in SiO_2 [101]) or Si—C (in SiC [120]), exhibit distinctive resonance effects at certain MIR wavelengths due to the strong coupling between incident photons and vibrational modes of their polar lattice structures. This resonance selectively enhances emissivity within a narrow spectral range, enabling precise spectral control of thermal radiation. Importantly, SPhPs occur selectively in materials exhibiting polar bonding characteristics. In contrast, non-polar materials such as carbon black exhibit high emissivity primarily through broadband intrinsic absorption and scattering mechanisms. Carbon black, for instance, owes its high emissivity to its disordered, porous, and graphitic microstructure, rather than resonance-based polaritonic coupling. Thus, the spectral selectivity offered by SPhP-based materials provides unique advantages in designing radiative cooling structures capable of targeted emission within specific atmospheric windows.

4.5 | Periodic Structure of the Device

Photonic devices with periodic structures play a crucial role in radiative cooling by selectively controlling light absorption, emission, and reflection (Figure 2e) [30]. Micro resonators, also known as optical microcavities, are a type of photonic structure that confines and manipulates light within a small space, enabling precise spectral control of thermal radiation [121]. This depends on their size [122], shape [123], and refractive index [124], which determine their optical response and interaction with incident light. Various photonic structures, including periodic arrays [122], diffraction gratings [125], conical pillar arrays [126], Fabry–Pérot cavity [127], multilayer pyramidal nanostructures [128], and dielectric resonators [129], are employed to regulate heat dissipation into the atmosphere. For example, spoof surface plasmon polaritons (sSPPs), realized through subwavelength periodic patterning on conductive surfaces, represent a class of engineered surface modes that fall under this structured-emitter category [130]. These geometrically defined dispersion modes enable narrowband mid-infrared thermal emission and are particularly valuable for designing compact and spectrally tunable radiators [131]. These structures can be tuned in terms of their dimensions and material composition to achieve high reflectivity across the solar spectrum while maximizing their emittance in the MIR range, optimizing their radiative cooling performance [100].

4.6 | IR Emissions of Molecules

Broadband IR emission is primarily governed by the vibrational and rotational transitions of chemical bonds or functional groups within materials (Figure 2f) [102]. The bending and stretching vibrations of organic molecular bonds typically occur in the spectral range of 400–4000 cm^{-1} (2.5–25 µm) [102], with specific absorption features such as C═O (5.8 µm) [132], C─O (7.7–10 µm) [133], and C─H (7.8–14.5 µm) [133]. To minimize parasitic heat absorption, functional groups that emit within the atmospheric transparency window (8–13 µm, in Section 2), such as F─C─F (~8.4 µm) [134], ─CF_3 (9 µm) [135], Si─C (13.5 µm) [136], and Si─O─C (8.7–10.5 µm) [137], should be preserved to enhance cooling efficiency [138]. Additionally, as discussed in Section 3.2, thermal emission increases with temperature, meaning that higher device temperatures lead to more effective radiative cooling [139].

5 | Strategies for Energy Saving and Generation

5.1 | Reconfigurable Photonics for Temperature Regulation

Radiative thermal management technologies such as radiative cooling and solar heating are crucial for leveraging thermal radiation between space and the sun to conserve energy. Radiative cooling employs the cold temperatures of outer space (approximately 3 K) as a heat sink, enabling cooling without energy consumption by applying principles from Planck's law, which states that all physical bodies emit electromagnetic waves [140–143]. This method is particularly effective because of an atmospheric window between 8 and 13 µm, where electromagnetic waves can pass effectively, allowing objects on Earth with an ambient temperature of around 300 K to efficiently absorb and emit radiation [40, 139]. Solar energy, which constitutes 99.9% of Earth's sustainable energy, also plays a vital role in zero-energy thermoregulation through efficient radiative solar heating. However, the passive nature of these technologies can lead to inefficiencies, such as unwanted cooling in winter or excessive heating in summer, necessitating additional energy use, especially under dynamically changing climate conditions [21, 144]. To address these limitations, Figure 3a illustrates that switchable radiative thermal management technologies have been developed. Across various applications spanning a broad spectral range, multiple materials enable switchable light–matter interactions [149–150], including swelling [151–155], carrier pumping [156], thermochromic [157–158], and electrochromic mechanisms [104, 159–161]. These materials facilitate the transition between sub-ambient cooling and above-ambient heating by modifying optical properties in the solar or IR wavelength regions, thereby improving thermal management efficiency with minimal energy consumption.

5.1.1 | Adaptive Photonics via Phase Transition Materials

Recent advancements in radiative thermal management have introduced temperature-adaptive coatings and smart window technologies for efficient all-season thermal regulation. As shown in Figure 3b, Tang et al. [29] experimentally demonstrated a temperature-adaptive radiative coating for household thermal management by lowering the phase-transition temperature of $W_xV_{1-x}O_2$ to approximately 22°C. Below this transition temperature, the material remains in an insulating state, enabling a heating mode. When the temperature exceeds the transition point, its metallic properties enhance absorption, enabling radiative cooling.

Another approach, based on phase-change materials (PCM), introduced a smart window system designed for energy-efficient building applications with tunable emissivity in the atmospheric window (Figure 3c) [145]. This system, utilizing a W-doped VO_2-Polymethyl methacrylate (PMMA)/spacer/low-E stack, offers scalable and solution-process-based thermal modulation to adapt to varying climatic conditions. The smart window modulates both NIR transmittance and heat emissivity to regulate indoor temperatures. During summer, it blocks NIR radiation, strongly emits LWIR radiation, and allows visible light to pass through. In winter, both NIR and visible light enter the room while heat radiation is suppressed, effectively maintaining indoor warmth.

5.1.2 | Electro-Optic Tuning of Solar Absorption and Thermal Radiation

Sui et al. [146] enhanced the emissivity in LWIR modulation of an electrochromic device (ECD) by incorporating Pt into the working electrode (Figure 3d). Unlike prior studies where Cu particles were sparsely distributed on bare graphene, the Pt modification reduced adsorption energy, leading to a denser and more uniform Cu deposition. This structural refinement improved electromagnetic wave reflection, achieving the highest reported emissivity modulation in LWIR (74%–85%) among thermochromic and electrochromic thermal management devices (Figure 3e). The radiative thermal management performance of the device was evaluated by estimating annual energy savings across 15 cities, with reductions ranging from 5 to 60 MBtu. The findings demonstrated that dynamic radiative thermal management is particularly effective in climates with significant daily and seasonal temperature fluctuations. Yang et al. [147] developed a bi-layer phase change material-enhanced radiative cooler (PCMRC) (Figure 3f) for adaptive temperature regulation. During the day, the PCM layer absorbs excess heat from

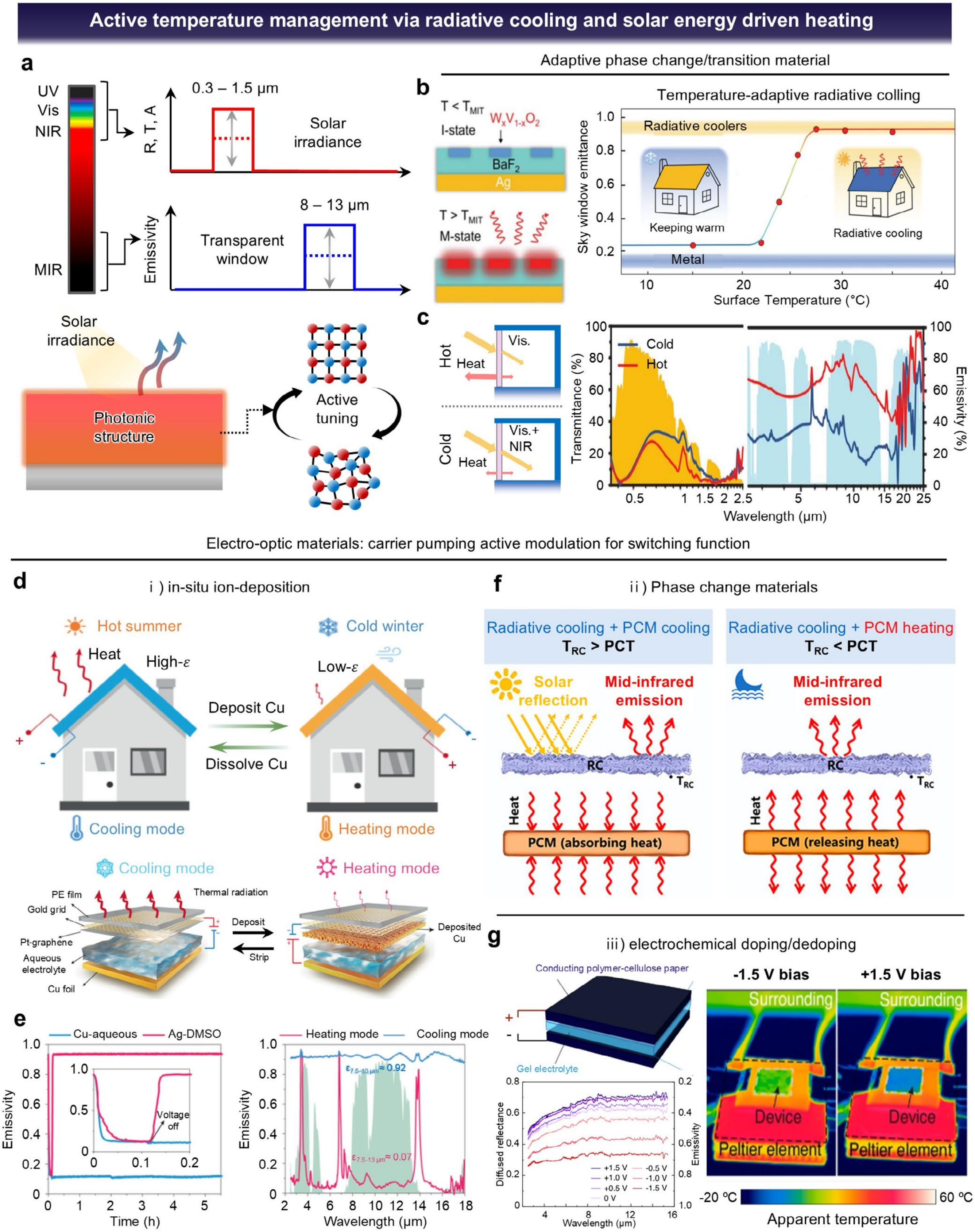

FIGURE 3 | Legend on next page.

FIGURE 3 | Active photonics for temperature management. (a) Schematic of spectrum intensity control based on reconfigurable photonics across wavelength bands. (b) Temperature-adaptive radiative cooler utilizing $W_xV_{1-x}O_2$ that actively alternates between insulating to retain warmth and radiating to cool. Reproduced with permission: Copyright 2021, American Association for the Advancement of Science [29]. (c) Thermochromic smart window based on VO_2, designed to regulate between insulation for warmth and radiative cooling. Reproduced with permission: Copyright 2021, American Association for the Advancement of Science [145]. (d) Schematic of emissivity control using an in situ ion-deposition method. Reproduced with permission: Copyright 2023, Springer Nature [146]. (e) Emissivity variation corresponding to the state of Cu-ion deposition and its impact on cooling performance. Reproduced with permission: Copyright 2023, Springer Nature [146]. (f) Phase change material-based control of emissivity and adjustment of solar absorptance. Reproduced with permission: Copyright 2023, American Chemical Society [147]. (g) Electrochemical doping and dedoping for emissivity control. Reproduced with permission: Copyright 2024, Springer Nature [148].

the radiative cooling (RC) layer, and at night, it releases stored heat. This process achieved an average temperature reduction of 6.3°C during the day and a 2.1°C increase at night, enabling both cooling and warming effects. Meanwhile, electrochemical doping can also modify the complex refractive index with low power consumption. Kuang et al. [148] demonstrated broadband emissivity tuning by more than 0.38, controlled through the electrochemical tuning of poly(3,4-ethylenedioxythiophene) (PEDOT) redox states (Figure 3g). When the device was turned off in a low-conducting state, the normalized reflectance gradually increased over approximately 20 min, stabilizing at an intermediate value (50% of the total reflectance range). Additionally, Li-doped WO_3 has shown a remarkable emissivity modulation ($\Delta\varepsilon_{\max} \approx 0.76$), further highlighting the potential of electrochromic materials as promising candidates for tunable thermal management systems [162].

Notably, the final reflectance state depended on whether the device was left unbiased from a high- or low-conductivity state, indicating an optical memory effect. This property not only enables low-power operation but also allows modulation of specular IR reflectance and thermal emissivity by approximately 40% with a low electrical bias of ±1.5 V, making it one of the most efficient IR-tunable materials.

5.2 | Thermoelectric Generation via Temperature Control

A solid-state thermoelectric generator (TEG) employs the Seebeck effect to convert temperature gradients into electrical power, offering mechanical stability, scalability, and durability [163]. Efforts to enhance TEG performance focus on increasing the temperature difference between its hot and cold ends, typically through heating or cooling (Figure 4a). Solar energy, Earth's primary thermal source, is extensively utilized for heating in passive TEG systems, with SA-based devices efficiently converting solar energy into electricity. For cooling, space at a chilly 3 K provides a natural source, enabling surfaces facing the sky to emit thermal radiation and reach subambient temperatures through radiative cooling. This process aids in passive electricity generation when integrated into a TEG. To overcome the limited temperature difference in passive RC-TEDs, researchers have developed RC-SA-TEDs, which combine solar absorbers and radiative coolers. Initially, Zhao et al. [164] proposed a vertically stacked RC-SA-TED. Later, Zhang et al. [169] demonstrated a sandwich-type TED (SA-TEG-RC) that achieved 24 h electricity generation, though partial shielding reduced its efficiency. Gao et al. [170] addressed this by reversing the structure (RC-TEG-SA), enhancing both cooling and the temperature gradient. To further mitigate shielding issues, Liao et al. [165] introduced a lateral configuration (SA-TEG-RC), placing the solar absorber and radiative cooler side by side. This lateral setup achieved temperature gradients exceeding 10°C between the absorber and cooler components, generating thermovoltages greater than 60 mV under moderate solar irradiance (~400 W m^{-2}) [165]. Wang et al. [171] took this a step further by integrating a greenhouse structure (RC-TEG-GH), which stabilized the temperature difference and enhanced the TED's performance for continuous energy harvesting (Figure 4b). Experimental data demonstrated that the system enabled fully passive, all-day power generation with an output of 90.74 mW m^{-2} [171].

5.2.1 | Bio-Inspired Dual-Mode TEGs

Han et al. [166] developed a stretchable dual-mode TEG with zebra stripe-like radiation modulators, forming alternating cooling and heating regions to enhance the in-plane temperature gradient (Figure 4c). By integrating passive daytime radiative cooling (PDRC) and solar heating, the device enabled continuous 24-h electricity generation, achieving a 24°C temperature difference during the day and 2.8°C at night. The device demonstrated power outputs of ~0.003 to 40 mW/m^2 with strong mechanical durability, highlighting its potential for scalable renewable energy systems. To achieve large-area implementation, Figure 4d presents scalable radiation-modulated thermoelectric fabrics for efficient thermal energy harvesting [167]. By optimizing the coverage ratio of a poly(vinylidene fluoride-co-hexafluoropropylene) (PVDF-HFP) fiber membrane on carbon nanotube (CNT)-based arrays, these fabrics enhanced thermal-to-electrical conversion, achieving a 37 K temperature gradient under 1-sun irradiation and an output voltage density of 6.67 V/m^2 at 800 W/m^2, demonstrating feasibility for large-scale solar thermoelectric applications.

5.2.2 | Wearable TEGs

Wearable TEGs utilizing body heat have emerged as a promising solution for self-powered electronics. However, the limited temperature difference between the hot and cold ends constrains their efficiency. Enhancing thermal radiation at the cold end has been explored as an effective approach to increase the temperature gradient and improve power output. To address this, Figure 4e presents a bio-inspired flexible thermal emitter designed to enhance radiative cooling through a multi-scale structure [156]. The emitter consists of a polydimethylsiloxane (PDMS) base, an Ag interlayer, and a PDMS-Al_2O_3 hybrid matrix with surface pyramid arrays,

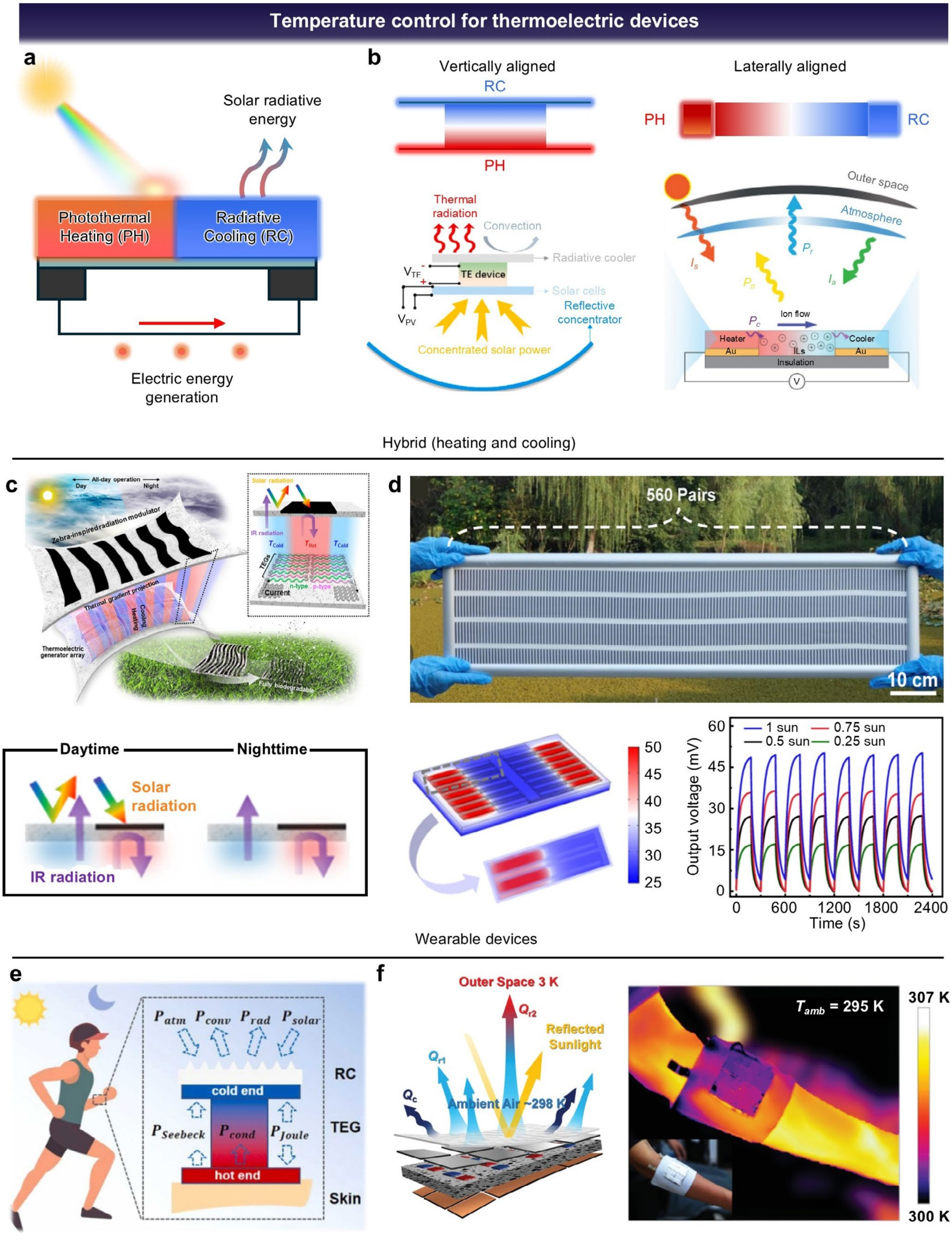

FIGURE 4 | Legend on next page.

FIGURE 4 | Temperature control for thermoelectric devices. (a) Schematic of thermoelectric generation (TEG) based on the temperature difference between the ends of the TEG. (b) Structural types of TEGs, illustrating vertically structured (left), Reproduced with permission: Copyright 2021, Elsevier [164], and planar structures (right) Reproduced with permission: Copyright 2023, Wiley [165], along with strategies for heating (photothermal effect) and cooling (radiative cooling). (c) Zebra stripe emissivity/absorptive patterns that induce substantial in-plane temperature gradients for thermoelectric power generation. Reproduced with permission: Copyright 2023, American Association for the Advancement of Science [166]. (d) Large-area thermoelectric generator featuring zebra stripe patterns for enhanced thermal management. Reproduced with permission: Copyright 2025, American Association for the Advancement of Science [167]. (e) Schematic of a wearable, vertically aligned TEG for passive energy generation. Reproduced with permission: Copyright 2024, Elsevier [156]. (f) Schematic and IR camera image of a wearable TEG with passive radiative cooler. Reproduced with permission: Copyright 2022, Wiley-VCH Verlag GmbH [168].

optimizing spectral properties for improved cooling performance. In the radiative cooling-based circular-TEG (RC-C-TEG), an increased radiative cooling area ($\alpha = 2.7$) resulted in an output voltage of 4.2 mV, representing a 150% improvement over conventional RC-TEGs ($\alpha = 1$). The impact of radiative cooling on TEG performance was further examined under different environmental conditions (Figure 4f) [168]. Experimental validation demonstrated that the integration of a radiative cooling coating led to a 128% increase in output power in exposed environments and a 96% increase in non-exposed conditions. Additionally, indoor tests at 295 K indicated a stable power density of 5.5 μW/cm^2, doubling that of uncoated devices. These findings highlight the potential of passive radiative cooling in significantly enhancing TEG efficiency across various operating conditions. While current efforts focus on enhancing the temperature gradient via radiative cooling structures integrated into TEGs, additional strategies that account for skin thermal conditions are essential for practical wearable applications. For example, Zheng et al. [172] developed a skin-conformal photonic patch that combines radiative and nonradiative heat transfer, achieving a temperature reduction of over 56°C under simulated solar and thermal loads. Such advances in thermal interface design could guide the development of wearable TEG systems by improving user comfort and device stability, particularly in outdoor or high-temperature environments.

5.3 | Photothermal Effect-Driven Water Evaporation

Evaporation occurs when solar radiation heats water and objects on Earth, allowing water molecules to absorb energy and gain sufficient kinetic energy to transition into vapor [76, 173]. This process is used in freshwater production [174], steam sterilization [175], fuel generation [176], and electricity production [177], primarily relying on photothermal effects. However, conventional solar-driven vapor generation systems suffer from heat dissipation when operated in bulk water, leading to efficiency losses [76, 173]. Therefore, interfacial solar evaporation systems position light-absorbing structures at the water-air interface (Figure 5a) [76, 173]. This system consists of a broadband absorption device, a substrate, and bulk water. The absorber captures incident light and converts it into heat, while the substrate transports water to the evaporating surface via capillary forces. However, heat loss by conduction to bulk water, radiation, and convection limits efficiency. To further enhance the performance, the system requires efficient light-to-heat conversion [178, 181], thermal insulation [182], and effective water transport of the substrate [180] (Figure 5ai–iii).

5.3.1 | Efficient Light-to-Heat Conversion

Maximizing light-to-heat conversion requires enhancing solar photon capture through multiple scattering and reabsorption (Figure 5ai,b) [183]. This broadband absorber containing graphite is designed by mimicking the porous morphology of *Cyprinid* fish scales [178]. It features vertical macropores (240–360 μm) and interconnected micropores (30–60 μm), achieving ~97% solar absorption (Figure 5c). With a light intensity of just 0.2 W/cm^2, it enables uniform heating up to 80°C (Figure 5d). While contact solar absorption provides a high evaporation rate, it faces challenges such as salt contamination and efficiency degradation over time. Advanced interfacial designs are necessary to mitigate these limitations to sustain long-term stability and optimize photothermal efficiency.

5.3.2 | Thermal Insulation

A contact evaporator directly interfaces the solar absorber with water, while a non-contact evaporator incorporates a gap to separate bulk water [184]. Although contact systems achieve high evaporation rates, they suffer from salt accumulation and efficiency loss over time [185]. In contrast, non-contact systems prevent contamination but remain susceptible to heat dissipation through conduction, convection, and radiation, particularly in bulk water [186]. To address this issue, thermal insulation is introduced by incorporating a confined water layer that enables both localized solar absorption and thermal insulation (Figure 5aii,e) [179]. Under uniform sunlight illumination (1000 W/m^2), the confined water layer maintains a steady-state temperature of ~40°C while effectively evaporating 3.5 wt% brine (Figure 5f). Over 7 days' operation, no salt crystallization is observed, demonstrating a stable solar-to-vapor conversion efficiency of 67% (Figure 5g). This approach minimizes heat loss, enhances evaporation efficiency, and ensures long-term operational stability in solar-driven water evaporation systems.

5.3.3 | Efficient Water Transport

Efficient water transport is essential for sustaining interfacial solar evaporation by ensuring a continuous supply of water [187–188], effective salt transport [189], and localized heat

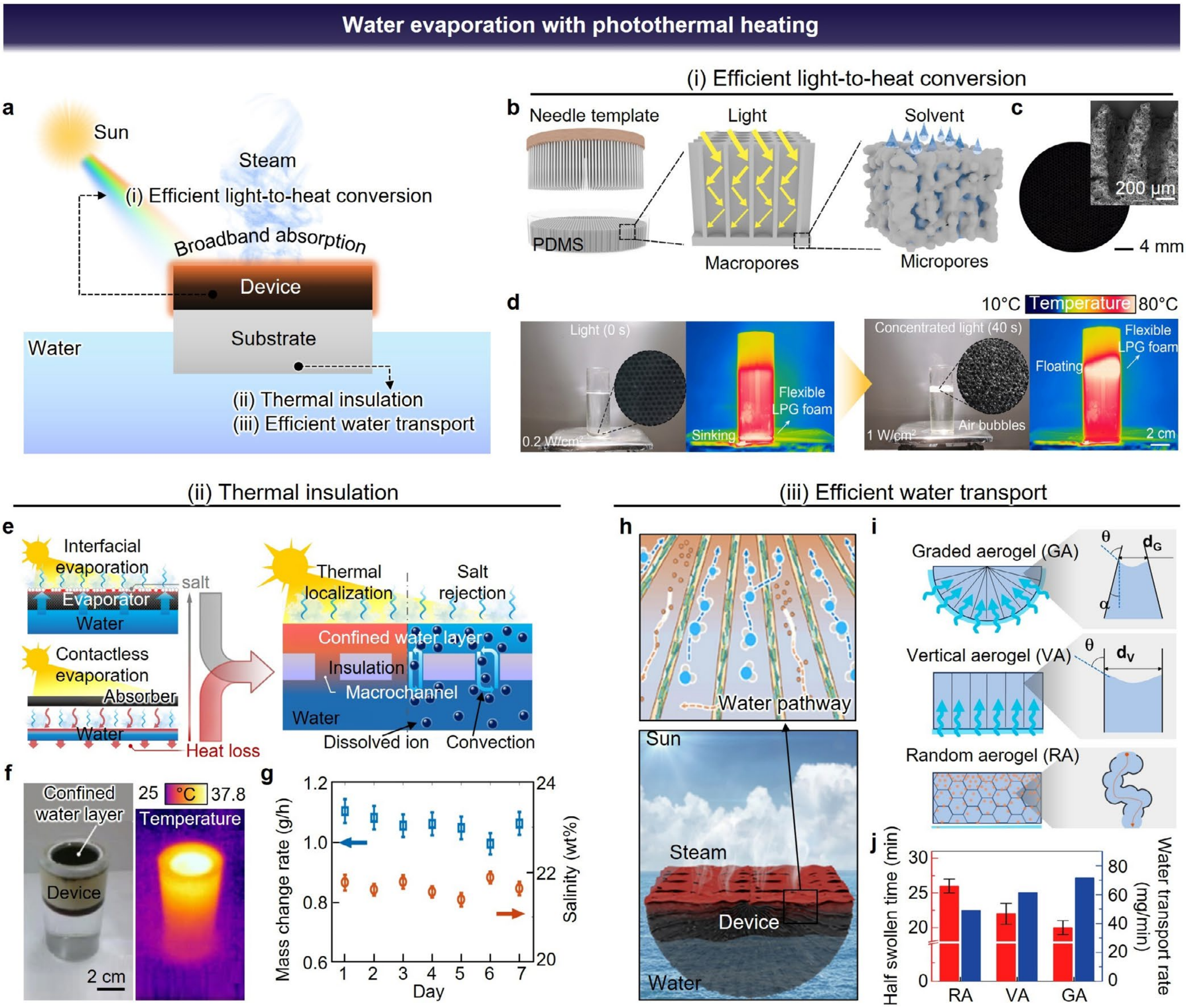

FIGURE 5 | Water evaporation with photothermal heating. (a) Interfacial solar evaporation, highlighting key components: (i) efficient light-to-heat conversion, (ii) thermal insulation, and (iii) effective water transport. (b) Broadband photothermal absorber mimicking *Cyprinid* fish scales for enhanced solar absorption by multiple scattering and reabsorption. (c) Corresponding photograph and SEM image. (d) The heating characteristics of the absorber under solar illumination. Reproduced with permission: Copyright 2024, American Association for the Advancement of Science [178]. (e) Simultaneous thermal insulation and salt removal through a confined water layer structure. (f) The thermal insulation performance of the confined water layer structure. (g) Stability test results over 1 week of daily 8-h evaporation cycles with 20 wt% brine. Reproduced with permission: Copyright 2022, Springer Nature [179]. (h) Fan-shaped aerogel with a hierarchical porous structure, inspired by tree-like transport systems. (i) Schematic design of an improved water transport mechanism enabled by a hierarchical structure, and (j) analysis of the resulting half-expansion time and water transport rate. Reproduced with permission: Copyright 2024, Springer Nature [180].

retention (Figure 5aiii) [190]. Therefore, enhancing water transport pathways is essential for maintaining system stability. For example, inspired by tree-like capillary transport systems, a fan-shaped aerogel has been engineered to enhance solar absorption while minimizing conductive heat loss (Figure 5f,i) [180]. This structure incorporates a hierarchical porous network, facilitating efficient water transport while mitigating localized drying and salt deposition. Consequently, the system achieves a stable evaporation rate of 2.09 $kg/m^2 h^{-1}$ under continuous daily illumination in a 3.5 wt% NaCl solution over 7 days without observable degradation (Figure 5j).

5.4 | Thermal-Promoted Catalysts

Photocatalysis and photothermal catalysis harness solar energy to drive chemical reactions, converting it into chemical energy [191]. Optimizing the thermal environment around catalysts can significantly enhance their efficiency (Figure 6a). Heat-promoted catalytic enhancement provides three key benefits: improved mass transfer (Figure 6ai), reduction in apparent activation energy (Figure 6aii), and increased reactants in excited states (Figure 6aiii). First, elevated temperatures enhance reactant and product diffusion (Figure 6ai), accelerating

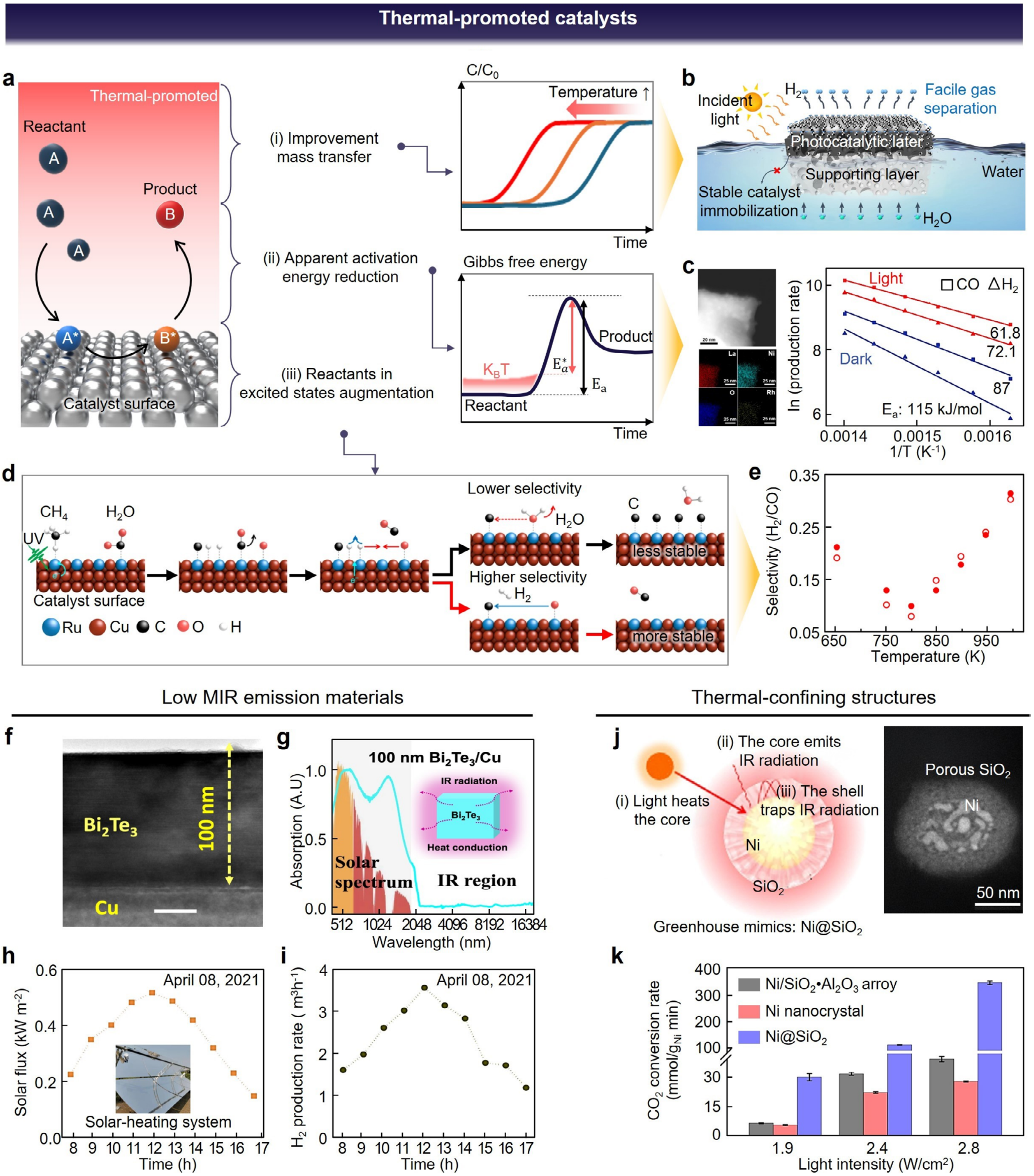

FIGURE 6 | Thermal-promoted catalysts. (a) Overview of thermal-promoted catalytic processes, highlighting key benefits: (i) improved mass transfer, (ii) reduction in apparent activation energy, and (iii) increased reactants in excited states. (b) Enhanced water vapor diffusion for hydrogen production. Reproduced with permission: Copyright 2023, Springer Nature [192]. (c) Heat-induced reduction of apparent activation energy in CO and H_2 production. Reproduced with permission: Copyright 2023, Wiley-VCH Verlag GmbH [193]. (d) Increased excited-state reactants, (e) improving catalytic selectivity for H_2. Reproduced with permission: Copyright 2020, Springer Nature [194]. (f) The designed catalytic system with Bi_2Te_3/Cu heterostructure, (g) achieving high solar absorption and low IR emittance. (h) Measured solar flux of the large-area catalytic system (inset) under sunlight irradiation on April 8, 2021, in Baoding City, China. (i) Corresponding hydrogen production rate. Reproduced with permission: Copyright 2022, Springer Nature [28]. (j) Greenhouse-structured catalyst with a core-shell design for heat confinement. (k) CO_2 conversion performance of the Ni-SiO_2 catalyst. Reproduced with permission: Copyright 2021, Springer Nature [195].

reaction rates and improving efficiency [196]. For instance, increased water vapor diffusion can promote hydrogen production (Figure 6b) [192]. When thermal energy exceeds the apparent activation barrier of a catalytic reaction (Figure 6aii) [197], the apparent activation energy decreases, as higher temperatures elevate reactant energy levels. This effect has been demonstrated in reactions producing CO and H_2, where heat effectively lowers apparent activation energy (Figure 6c) [193]. Lastly, the excited state reactants increase (Figure 6aiii), preventing the byproducts production, leading to higher selectivity in catalytic reactions (Figure 6d,e) [194]. To maintain an optimal thermal environment, low-MIR-emission materials reduce heat loss [28], while thermal-confining structures help retain heat for improved catalytic efficiency [195].

5.4.1 | Low MIR Emission Materials

Minimizing MIR emission is a representative strategy for maintaining high temperatures around catalysts, as thermal radiation losses can significantly reduce reaction efficiency. Materials with low MIR emissivity can prevent excessive heat dissipation, ensuring localized heat retention for sustained catalytic activity. For example, a Bi_2Te_3/Cu heterostructure was designed to reduce IR emission and retain heat (Figure 6f) [28]. The optimized device, with a 100 nm Bi_2Te_3 film on Cu, achieved ~89% absorption in the 400–2000 nm solar range while maintaining a low IR emittance of 5% (Figure 6g). As a result, the temperature rapidly increased to 317°C under 1-sun irradiation. Even in a scalable system, high hydrogen production efficiency (1.19–3.56 m^3/h, Figure 6h) was achieved, depending on sunlight intensity (0.15–0.52 kW/m^2, Figure 6i), with a total daily hydrogen yield of 23.27 m^3, demonstrating strong industrial potential.

5.4.2 | Thermal-Confining Structures

Structures designed to confine heat effectively reduce conduction and convective losses, maintaining higher localized temperatures for prolonged catalytic activity. For instance, the greenhouse-structured catalyst with a core-shell design effectively traps heat from light-heated Ni nanoparticles (Figure 6j), minimizing thermal losses [195]. The porous SiO_2 shell acts as an insulating layer, slowing heat conduction to the surroundings while also trapping IR radiation emitted by the hot Ni core through absorption and scattering at the interface. This reduces thermal radiation by 43%, leading to a temperature increase. As a result, the catalyst achieved a CO_2 conversion rate of 0.344 mol g_{ni}^{-1} min^{-1} (20.6 mol g_{ni}^{-1} h^{-1}) at 2.8 W cm^{-2}, maintaining a higher local temperature for 10 min (Figure 6k). This catalytic system can further enhance thermal energy retention, leading to higher efficiency and improved selectivity in solar-driven catalytic reactions.

5.5 | Thermal Radiation Control for Enhanced Efficiency of PV Devices

Radiative cooling presents a valuable approach to enhance the performance of solar cells by mitigating heat accumulation. In silicon-based single-junction solar cells, electricity is generated through the PV effect [198]. However, due to the Shockley–Queisser limit, only about 33.7% of absorbed solar energy is converted into electricity; the remaining energy primarily turns into heat. This excess heat increases the operating temperature, potentially reducing both the efficiency and the lifespan of the cells. Additionally, elevated temperatures can lead to increased carrier recombination and reduced carrier lifetime, further decreasing solar power efficiency (Figure 7a) [204–205]. For example, crystalline silicon solar cells typically experience an efficiency loss of about 0.4%–0.5% for every 1°C increase in temperature [206]. Therefore, maintaining a lower temperature is essential for maximizing energy output. Zhu et al. [199] explored the relationship between solar illumination and temperature variations in solar cells at different temperatures. Figure 7b depicts a thermal simulation of a silicon solar cell with a silica overlay. The model incorporates radiative cooling and nonradiative heat dissipation through convection and conduction, as shown in the boundary condition:

$$-\kappa(z)\frac{dT(z)}{dz}\,|_{\text{top}} = P_{\text{cooling}}(T)_{\text{Emit}} + h_1\left((T)_{\text{Emit}} - T_{\text{amb}}\right) \qquad (6)$$

This boundary condition integrates the cooling effects of radiation and additional heat dissipation from convection and conduction, characterized by the coefficient h_1.

The lower surface is responsible for nonradiative heat loss as described by:

$$\kappa\frac{dT(z)}{dz}\,|_{\text{bottom}} = h_2\left((T)_{\text{bottom}} - T_{\text{amb}}\right) \qquad (7)$$

where k represents thermal conductivity, and $T(z)$ indicates the temperature distribution. The heat equation is solved iteratively until a self-consistent solution is achieved, stabilizing the upper surface temperature. The operating temperature of the solar cell is then determined as the spatial average of the temperature within the cell.

Given the annual wind and climate conditions in the United States, and a solar heating power of 800 W/m^2, the uncooled solar cell's temperature can be expected to rise approximately 42.3 K above ambient. This underscores the critical need for temperature management strategies such as radiative cooling.

5.5.1 | Enhanced Energy Harvesting Through Light Trapping and Radiative Cooling

Resonant interactions between electromagnetic radiation and materials with structural features on the wavelength scale of incident light have been well established. Such multi-dimensional structures provide opportunities to enhance optical performance. Perrakis et al. [64] introduced a nano- and micro-patterned radiative cooler designed to improve both radiative cooling and solar cell efficiency. The microstructure enhanced LWIR heat emission, while the nanostructures functioned as an anti-reflective coating in the solar spectrum. Their simulation results indicated a 3.1% increase in silicon solar cell efficiency and a 5.8°C

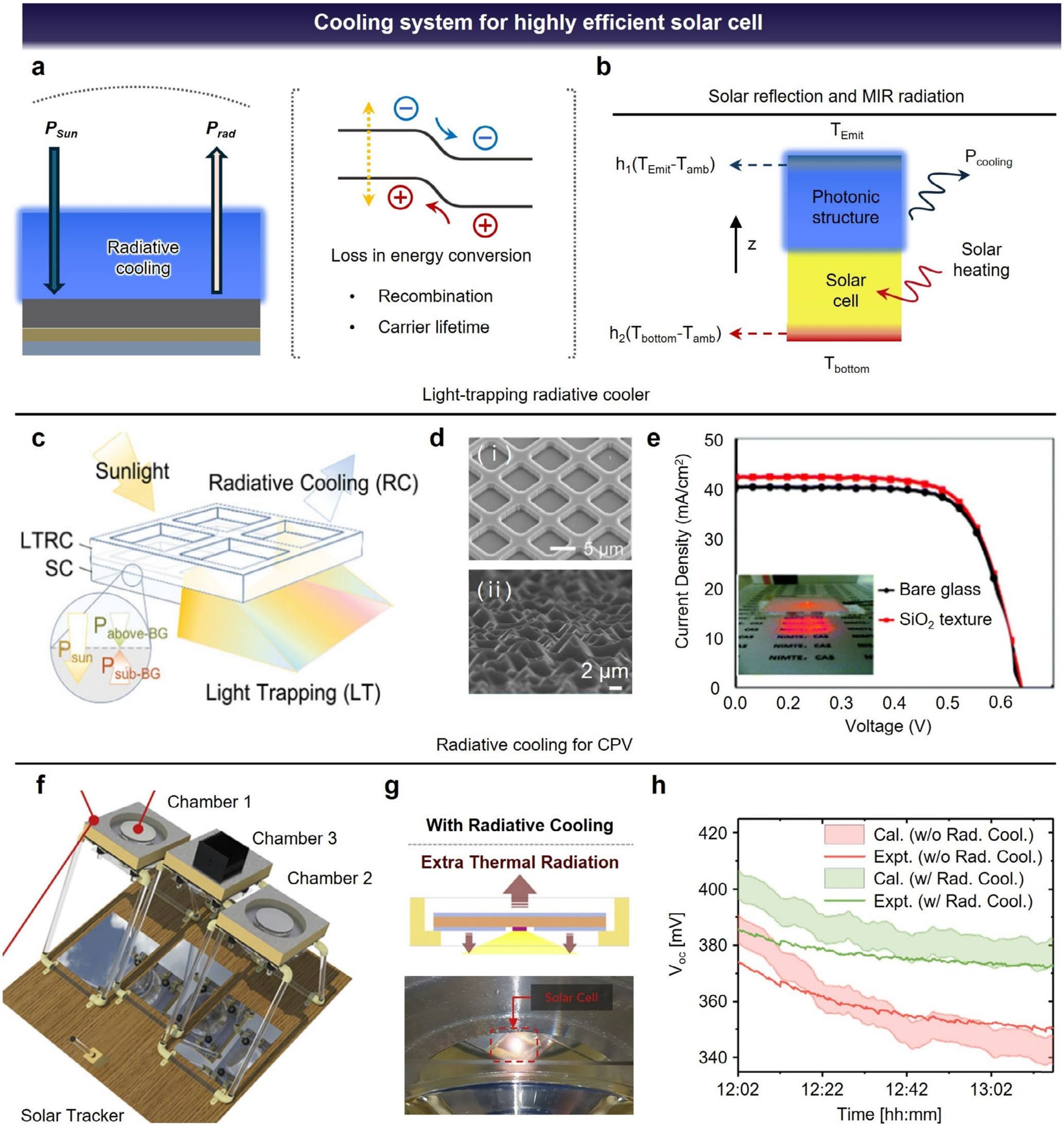

FIGURE 7 | Radiative cooling system for enhancing solar cell efficiency. (a) Schematic illustration of a passive radiative cooling system integrated with a solar cell, highlighting key factors reducing photovoltaic efficiency due to elevated temperatures. (b) Thermal simulation schematic with non-radiative heat exchange coefficients h_1 and h_2 at the upper and lower surfaces, respectively, and ambient temperature denoted as Tamb. Reproduced with permission: Copyright 2014, Optica Publishing Group [199]. (c) Illustration of a radiative cooler designed to simultaneously radiate heat and trap light. Reproduced with permission: Copyright 2021, Wiley-VCH Verlag GmbH [200]. (d) SEM image showing a scattered structure with (i) a 2D grating, Reproduced with permission: Copyright 2021, Wiley-VCH Verlag GmbH [200], and (ii) a disordered pyramid structure. Reproduced with permission: Copyright 2017, Wiley-VCH Verlag GmbH [201]. (e) Comparison of current density between control and textured glass, with an inset showing the transmission haze of SiO_2 textured glass. Reproduced with permission: Copyright 2017, Wiley-VCH Verlag GmbH [201]. (f) Photograph of electrodes and thermocouples attached to the solar cell. Reproduced with permission: Copyright 2020, Elsevier [202]. (g) Schematic and photograph of a radiative cooler integrated with a concentrated photovoltaic (CPV) system. Reproduced with permission: Copyright 2020, Elsevier [202]. (h) Real-time V_{OC} measurements indicating improved performance with radiative cooling (green curve) versus without (red curve), showing a V_{OC} increase of about 20 mV (5.7% relative increase). Reproduced with permission: Copyright 2019, Optica Publishing Group [203].

reduction in temperature. Recent studies have explored passive cooling integrated with solar radiation management. Heo et al. [200] developed a 2D SiO_2 metasurface that facilitated both radiative cooling and light trapping (Figure 7c). The metasurface exhibited broadband emissivity across the LWIR–FIR spectrum, resulting in a 6°C temperature reduction and a 1.3% efficiency improvement in an InGaP/GaAs/Ge multi-junction solar cell (MJSC). Outdoor field tests further validated the enhanced thermal and electrical performance of the metasurface-integrated MJSC compared to a conventional glass-mounted counterpart under direct sunlight (~900 W m^{-2}). Additionally, microstructures (Figure 7d) enhanced light scattering within the solar spectrum, increasing the optical path length in the absorption layer. Lu et al. [201] proposed ultra-broadband surface textures fabricated via a modified sol–gel imprinting method, enabling interaction with visible to FIR radiation (Figure 7e). Their study demonstrated that geometric diffraction within the solar spectrum enhanced short-circuit current by 5.12% and solar cell efficiency by 3.13%, further highlighting the potential of structured surfaces for improving PV performance.

5.5.2 | Radiative Cooling for Improved Performance in Concentrated Photovoltaics

Beyond individual solar cell cooling, radiative cooling has also been explored for system-level applications, including extraterrestrial PV systems, thermal PV systems, and concentrated photovoltaic (CPV) systems. Wang et al. [202] investigated the lightweight radiative cooling performance of CPV systems (Figure 7f), where electrodes and thermocouples were attached to solar cells in separate chambers to measure open-circuit voltage (V_{OC}). Figure 7g captures a focused light beam directed at the center of the solar cell. Outdoor experiments demonstrated that radiative cooling contributed 25%–62% of the total cooling power in a CPV system. Zhou et al. [203] further refined this approach by investigating radiative cooling in low-bandgap PV cells, relevant to CPV and thermophotovoltaic (TPV) applications. Their study demonstrated improved cooling performance in low-bandgap GaSb PV cells under concentrated sunlight. Real-time V_{OC} measurements indicated that the GaSb PV diode with a radiative cooler (solid green curve) maintained a higher V_{OC} than the diode without a radiative cooler (solid red curve) due to its lower operating temperature (Figure 7h).

6 | Conclusions and Outlook

Photonic platforms, spanning a broad spectrum of electromagnetic waves, play a crucial role in energy systems by enhancing energy production and conservation. This review presents a comprehensive approach to thermal management, integrating solar absorption and radiative cooling strategies within a unified photonic framework. By targeting key spectral regions, such as the sub-2 μm band for efficient solar energy capture and the 8–13 μm LWIR window for effective radiative cooling, photonic designs offer scalable and energy-efficient solutions for temperature regulation, thermoelectric generation, steam production, and photocatalysis. The findings presented in this review highlight the critical role of light–matter interactions in advancing next-generation energy technologies through tailored material and structural designs.

This review explores the fundamentals of photonic mechanisms that govern energy devices, bridging theoretical principles with practical applications. We first examine Earth's thermal energy dynamics, emphasizing how photonic structures manipulate heat exchange to enhance energy efficiency. These insights suggest that optimizing spectral selectivity and material properties through thermal management is key to maximizing energy device's performance in diverse operating conditions. Looking ahead, continued advances in photonic materials and architectures are expanding the capabilities of thermal management beyond traditional limits. Recent developments, such as optically reconfigurable metasurfaces utilizing PCMs for independent infrared and visible modulation [207], metasurfaces achieving polarization-selective and chiral thermal emission without external sources [208], and asymmetric directional thermal emitters [209], highlight the versatility and future potential of metasurface-based approaches. By leveraging such functionalities, photonic metasurfaces are expected to offer greater adaptability in controlling both light and heat flows, paving the way toward intelligent and environment-responsive thermal management platforms. Despite considerable progress in engineering photonic materials for energy applications, their practical deployment requires balancing spectral performance, environmental stability, and manufacturability. For example, multilayer dielectric structures enable sharp spectral selectivity for radiative cooling, but their fragility under thermal cycling and fabrication complexity limit large-scale use. In contrast, polymer-based coatings offer scalable and low-cost processing but suffer from photodegradation and limited thermal endurance [210]. These trade-offs must be strategically considered depending on the application context—including target temperature range, device area, and outdoor exposure. To aid this process, our review provides material-specific examples across photothermal and radiative cooling systems, offering practical guidelines for selecting suitable photonic platforms aligned with operational requirements.

We anticipate that further advancements in photonic materials and device architectures will enable the next generation of energy-efficient technologies, bridging the gap between sustainable energy harvesting and intelligent thermal management. Future research should focus on scalable fabrication techniques, multi-functional hybrid materials, and dynamic photonic architectures to push the boundaries of adaptive thermal regulation. Synergetic strategies that integrate photothermal heating and radiative cooling within unified photonic structures are expected to significantly enhance thermal control performance, enabling energy devices to maintain high efficiency and adaptability across a wide range of environmental conditions. As photonic platforms continue to evolve, their integration into energy systems will play a pivotal role in achieving greater efficiency, longevity, and environmental adaptability, addressing the growing challenges in thermal energy control and sustainability.

Author Contributions

J.H. Ko and D. Kim contributed equally to this work. They jointly conceived the review scope, conducted the literature analysis, and drafted

the manuscript. S.Y. Kim and Y.J. Na provided critical feedback and helped revise the manuscript. Y.M. Song and H.-H. Jeong supervised the project and guided the overall direction of the review.

Acknowledgments

This work was supported by the GIST-MIT Research Collaboration through a grant funded by the National Research Foundation of Korea (NRF) funded by the Ministry of Science and ICT (RS-2025-16902996, 2021M3H4A1A04086357). This work is also supported by the Technology Innovation Program (RS-2024-00467230) funded by the Ministry of Trade Industry & Energy (MOTIE, Korea). J.H.K. acknowledges the support from the NRF (RS-2024-00345558).

Conflicts of Interest

The authors declare no conflicts of interest.

References

1. X. Zheng and L. Zhang, "Photonic Nanostructures for Solar Energy Conversion," *Energy & Environmental Science* 9, no. 8 (2016): 2511–2532, https://doi.org/10.1039/C6EE01182A.

2. W. Wang and L. Qi, "Light Management With Patterned Micro- and Nanostructure Arrays for Photocatalysis, Photovoltaics, and Optoelectronic and Optical Devices," *Advanced Functional Materials* 29, no. 25 (2019): 1807275, https://doi.org/10.1002/adfm.201807275.

3. R. Baetens, B. P. Jelle, and A. Gustavsen, "Properties, Requirements and Possibilities of Smart Windows for Dynamic Daylight and Solar Energy Control in Buildings: A State-Of-The-Art Review," *Solar Energy Materials & Solar Cells* 94, no. 2 (2010): 87–105, https://doi.org/10.1016/j.solmat.2009.08.021.

4. G. D. Scholes, G. R. Fleming, A. Olaya-Castro, and R. van Grondelle, "Lessons From Nature About Solar Light Harvesting," *Nature Chemistry* 3, no. 10 (2011): 763–774, https://doi.org/10.1038/nchem.1145.

5. T. Deppe and J. N. Munday, "Nighttime Photovoltaic Cells: Electrical Power Generation by Optically Coupling With Deep Space," *ACS Photonics* 7, no. 1 (2020): 1–9, https://doi.org/10.1021/acsphotonics.9b00679.

6. L. Zhou, H. Song, N. Zhang, et al., "Hybrid Concentrated Radiative Cooling and Solar Heating in a Single System," *Cell Reports Physical Science* 2, no. 2 (2021): 100338, https://doi.org/10.1016/j.xcrp.2021.100338.

7. B. Zhao, M. Hu, X. Ao, Q. Xuan, and G. Pei, "Spectrally Selective Approaches for Passive Cooling of Solar Cells: A Review," *Applied Energy* 262 (2020): 114548, https://doi.org/10.1016/j.apenergy.2020.114548.

8. M. Gao, C. K. Peh, L. Zhu, G. Yilmaz, and G. W. Ho, "Photothermal Catalytic Gel Featuring Spectral and Thermal Management for Parallel Freshwater and Hydrogen Production," *Advanced Energy Materials* 10, no. 23 (2020): 2000925, https://doi.org/10.1002/aenm.202000925.

9. M. B. Hayat, D. Ali, K. C. Monyake, L. Alagha, and N. Ahmed, "Solar Energy—A Look Into Power Generation, Challenges, and a Solar-Powered Future," *International Journal of Energy Research* 43, no. 3 (2019): 1049–1067, https://doi.org/10.1002/er.4252.

10. V. Fthenakis, J. E. Mason, and K. Zweibel, "The Technical, Geographical, and Economic Feasibility for Solar Energy to Supply the Energy Needs of the US," *Energy Policy* 37, no. 2 (2009): 387–399, https://doi.org/10.1016/j.enpol.2008.08.011.

11. C. Wang, S. Yu, X. Guo, et al., "Maximizing Solar Energy Utilization Through Multicriteria Pareto Optimization of Energy Harvesting and Regulating Smart Windows," *Cell Reports Physical Science* 1, no. 7 (2020): 100108, https://doi.org/10.1016/j.xcrp.2020.100108.

12. K. W. Lee, W. Lim, M. S. Jeon, et al., "Visibly Clear Radiative Cooling Metamaterials for Enhanced Thermal Management in Solar Cells and Windows," *Advanced Functional Materials* 32, no. 1 (2022): 2105882, https://doi.org/10.1002/adfm.202105882.

13. D. Zhao, A. Aili, Y. Zhai, et al., "Radiative Sky Cooling: Fundamental Principles, Materials, and Applications," *Applied Physics Reviews* 6, no. 2 (2019): 21306, https://doi.org/10.1063/1.5087281.

14. G. Huang, A. R. Yengannagari, K. Matsumori, et al., "Radiative Cooling and Indoor Light Management Enabled by a Transparent and Self-Cleaning Polymer-Based Metamaterial," *Nature Communications* 15, no. 1 (2024): 3798, https://doi.org/10.1038/s41467-024-48150-2.

15. K. C. S. Ly, X. Liu, X. Song, et al., "A Dual-Mode Infrared Asymmetric Photonic Structure for All-Season Passive Radiative Cooling and Heating," *Advanced Functional Materials* 32, no. 31 (2022): 2203789, https://doi.org/10.1002/adfm.202203789.

16. H. Kwak, D. H. Kim, and Y. M. Song, "Design of Double-Sided Optical Coatings for Space Cooling Through Vertical Windows," *Advanced Photonics Research* 6 (2025): 2400205, https://doi.org/10.1002/adpr.202400205.

17. X. Xue, M. Qiu, Y. Li, et al., "Creating an Eco-Friendly Building Coating With Smart Subambient Radiative Cooling," *Advanced Materials* 32, no. 42 (2020): 1906751, https://doi.org/10.1002/adma.201906751.

18. L. Zhu, A. P. Raman, and S. Fan, "Radiative Cooling of Solar Absorbers Using a Visibly Transparent Photonic Crystal Thermal Blackbody," *Proceedings of the National Academy of Sciences* 112, no. 40 (2015): 12282–12287, https://doi.org/10.1073/pnas.1509453112.

19. D. H. Kim, S. Y. Heo, Y. W. Oh, et al., "Polarization-Mediated Multi-State Infrared System for Fine Temperature Regulation," *APL Photonics* 8, no. 3 (2023): 30801, https://doi.org/10.1063/5.0136842.

20. X. Ao, B. Li, B. Zhao, et al., "Self-Adaptive Integration of Photothermal and Radiative Cooling for Continuous Energy Harvesting From the Sun and Outer Space," *Proceedings of the National Academy of Sciences* 119, no. 17 (2022): e2120557119, https://doi.org/10.1073/pnas.2120557119.

21. X. Li, B. Sun, C. Sui, et al., "Integration of Daytime Radiative Cooling and Solar Heating for Year-Round Energy Saving in Buildings," *Nature Communications* 11, no. 1 (2020): 6101, https://doi.org/10.1038/s41467-020-19790-x.

22. Y. Zhu, H. Luo, C. Yang, et al., "Color-Preserving Passive Radiative Cooling for an Actively Temperature-Regulated Enclosure," *Light: Science & Applications* 11, no. 1 (2022): 122, https://doi.org/10.1038/s41377-022-00810-y.

23. S. Zeng, S. Pian, M. Su, et al., "Hierarchical-Morphology Metafabric for Scalable Passive Daytime Radiative Cooling," *Science* 373, no. 6555 (2021): 692–696, https://doi.org/10.1126/science.abi5484.

24. S. Gamage, E. S. H. Kang, C. Åkerlind, et al., "Transparent Nanocellulose Metamaterial Enables Controlled Optical Diffusion and Radiative Cooling," *Journal of Materials Chemistry C* 8, no. 34 (2020): 11687–11694, https://doi.org/10.1039/D0TC01226B.

25. W. Luo, X. Xuan, J. Shen, et al., "High Performance Photothermal Carbon Nanotubes/Nanostructured Hydrogel for Solar Electricity Production and Solar Water Sterilization," *Applied Surface Science* 643 (2024): 158680, https://doi.org/10.1016/j.apsusc.2023.158680.

26. Y. Guo, Y. Sui, J. Zhang, Z. Cai, and B. Xu, "An All-Day Solar-Driven Vapor Generator via Photothermal and Joule-Heating Effects," *Journal of Materials Chemistry A* 8, no. 47 (2020): 25178–25186, https://doi.org/10.1039/D0TA08329A.

27. G. Fan, R. Ning, X. Li, et al., "Mussel-Inspired Immobilization of Photocatalysts With Synergistic Photocatalytic–Photothermal Performance for Water Remediation," *ACS Applied Materials &*

Interfaces 13, no. 26 (2021): 31066–31076, https://doi.org/10.1021/acsami.1c02973.

28. Y. Li, X. Bai, D. Yuan, et al., "General Heterostructure Strategy of Photothermal Materials for Scalable Solar-Heating Hydrogen Production Without the Consumption of Artificial Energy," *Nature Communications* 13, no. 1 (2022): 776, https://doi.org/10.1038/s41467-022-28364-y.

29. K. Tang, K. Dong, J. Li, et al., "Temperature-Adaptive Radiative Coating for All-Season Household Thermal Regulation," *Science* 374, no. 6574 (2021): 1504–1509, https://doi.org/10.1126/science.abf7136.

30. A. P. Raman, M. A. Anoma, L. Zhu, E. Rephaeli, and S. Fan, "Passive Radiative Cooling Below Ambient Air Temperature Under Direct Sunlight," *Nature* 515, no. 7528 (2014): 540–544, https://doi.org/10.1038/nature13883.

31. F. Esmaeilion, A. Ahmadi, S. Hoseinzadeh, M. Aliehyaei, S. A. Makkeh, and D. Astiaso Garcia, "Renewable Energy Desalination; a Sustainable Approach for Water Scarcity in Arid Lands," *International Journal of Sustainable Engineering* 14, no. 6 (2021): 1916–1942, https://doi.org/10.1080/19397038.2021.1948143.

32. L. Hammarström and S. Hammes-Schiffer, "Artificial Photosynthesis and Solar Fuels," *Accounts of Chemical Research* 42, no. 12 (2009): 1859–1860, https://doi.org/10.1021/ar900267k.

33. A. Pirvaram, N. Talebzadeh, S. N. Leung, and P. G. O'Brien, "Radiative Cooling for Buildings: A Review of Techno-Enviro-Economics and Life-Cycle Assessment Methods," *Renewable and Sustainable Energy Reviews* 162 (2022): 112415, https://doi.org/10.1016/j.rser.2022.112415.

34. X. Wu, G. Y. Chen, G. Owens, D. Chu, and H. Xu, "Photothermal Materials: A Key Platform Enabling Highly Efficient Water Evaporation Driven by Solar Energy," *Materials Today Energy* 12 (2019): 277–296, https://doi.org/10.1016/j.mtener.2019.02.001.

35. S. So, J. Yun, B. Ko, et al., "Radiative Cooling for Energy Sustainability: From Fundamentals to Fabrication Methods Toward Commercialization," *Advancement of Science* 11, no. 2 (2024): 2305067, https://doi.org/10.1002/advs.202305067.

36. D. Chae, S. Son, H. Lim, P. H. Jung, J. Ha, and H. Lee, "Scalable and Paint-Format Microparticle–Polymer Composite Enabling High-Performance Daytime Radiative Cooling," *Materials Today Physics* 18 (2021): 100389, https://doi.org/10.1016/j.mtphys.2021.100389.

37. B. Ko, D. Lee, T. Badloe, and J. Rho, "Metamaterial-Based Radiative Cooling: Towards Energy-Free All-Day Cooling," *Energies* 12, no. 1 (2019): 89, https://doi.org/10.3390/en12010089.

38. H. Sun, F. Tang, Q. Chen, et al., "A Recyclable, Up-Scalable and Eco-Friendly Radiative Cooling Material for All-Day Sub-Ambient Comfort," *Chemical Engineering Journal* 455 (2023): 139786, https://doi.org/10.1016/j.cej.2022.139786.

39. S. Fan and W. Li, "Photonics and Thermodynamics Concepts in Radiative Cooling," *Nature Photonics* 16, no. 3 (2022): 182–190, https://doi.org/10.1038/s41566-021-00921-9.

40. T. Li, Y. Zhai, S. He, et al., "A Radiative Cooling Structural Material," *Science* 364, no. 6442 (2019): 760–763, https://doi.org/10.1126/science.aau9101.

41. Z. Li, Q. Chen, Y. Song, B. Zhu, and J. Zhu, "Fundamentals, Materials, and Applications for Daytime Radiative Cooling," *Advanced Materials Technologies* 5, no. 5 (2020): 1901007, https://doi.org/10.1002/admt.201901007.

42. D. G. Baranov, Y. Xiao, I. A. Nechepurenko, A. Krasnok, A. Alù, and M. A. Kats, "Nanophotonic Engineering of Far-Field Thermal Emitters," *Nature Materials* 18, no. 9 (2019): 920–930, https://doi.org/10.1038/s41563-019-0363-y.

43. Z. Chen, L. Zhu, A. Raman, and S. Fan, "Radiative Cooling to Deep Sub-Freezing Temperatures Through a 24-h Day–Night Cycle," *Nature Communications* 7, no. 1 (2016): 13729, https://doi.org/10.1038/ncomms13729.

44. D. Li, X. Liu, W. Li, et al., "Scalable and Hierarchically Designed Polymer Film as a Selective Thermal Emitter for High-Performance All-Day Radiative Cooling," *Nature Nanotechnology* 16, no. 2 (2021): 153–158, https://doi.org/10.1038/s41565-020-00800-4.

45. X. Zhang, W. Yang, Z. Shao, et al., "A Moisture-Wicking Passive Radiative Cooling Hierarchical Metafabric," *ACS Nano* 16, no. 2 (2022): 2188–2197, https://doi.org/10.1021/acsnano.1c08227.

46. N. S. Bondareva, M. Sheikholeslami, and M. A. Sheremet, "The Influence of External Temperature and Convective Heat Exchange With an Environment on Heat Transfer Inside Phase Change Material Embedded Brick," *Journal of Energy Storage* 33 (2021): 102087, https://doi.org/10.1016/j.est.2020.102087.

47. J. Fan and L. Wang, "Review of Heat Conduction in Nanofluids," *Journal of Heat Transfer* 133, no. 4 (2011): 040801, https://doi.org/10.1115/1.4002633.

48. L. Li, S. Feng, Y. Bai, et al., "Enhancing Hydrovoltaic Power Generation Through Heat Conduction Effects," *Nature Communications* 13, no. 1 (2022): 1043, https://doi.org/10.1038/s41467-022-28689-8.

49. B. Buonomo, A. di Pasqua, O. Manca, and S. Nardini, "Evaluation of Thermal and Fluid Dynamic Performance Parameters in Aluminum Foam Compact Heat Exchangers," *Applied Thermal Engineering* 176 (2020): 115456, https://doi.org/10.1016/j.applthermaleng.2020.115456.

50. M. H. Mohammadi, H. R. Abbasi, A. Yavarinasab, and H. Pourrahmani, "Thermal Optimization of Shell and Tube Heat Exchanger Using Porous Baffles," *Applied Thermal Engineering* 170 (2020): 115005, https://doi.org/10.1016/j.applthermaleng.2020.115005.

51. F. P. Incropera, "Convection Heat Transfer in Electronic Equipment Cooling," *Journal of Heat Transfer* 110, no. 4b (1988): 1097–1111, https://doi.org/10.1115/1.3250613.

52. X. Chen, F. Wang, X. Yan, Z. Cheng, Y. Han, and Z. Jie, "Thermal and Chemical Analysis of Methane Dry Reforming in a Volumetric Reactor Under Highly Concentrated Solar Radiation," *Solar Energy* 162 (2018): 187–195, https://doi.org/10.1016/j.solener.2018.01.032.

53. Z. Zhou, Y. Fang, X. Wang, et al., "Synergistic Modulation of Solar and Thermal Radiation in Dynamic Energy-Efficient Windows," *Nano Energy* 93 (2022): 106865, https://doi.org/10.1016/j.nanoen.2021.106865.

54. X. Liu, L. Wang, and Z. M. Zhang, "Near-Field Thermal Radiation: Recent Progress and Outlook," *Nanoscale and Microscale Thermophysical Engineering* 19, no. 2 (2015): 98–126, https://doi.org/10.1080/15567265.2015.1027836.

55. D. D. L. Chung, "Materials for Thermal Conduction," *Applied Thermal Engineering* 21, no. 16 (2001): 1593–1605, https://doi.org/10.1016/S1359-4311(01)00042-4.

56. J. D. Jackson, "Fluid Flow and Convective Heat Transfer to Fluids at Supercritical Pressure," *Nuclear Engineering and Design* 264 (2013): 24–40, https://doi.org/10.1016/j.nucengdes.2012.09.040.

57. M. F. Modest and S. Mazumder, *Radiative Heat Transfer* (Academic Press, 2021).

58. Q. Wang, J. Warnan, S. Rodríguez-Jiménez, et al., "Molecularly Engineered Photocatalyst Sheet for Scalable Solar Formate Production From Carbon Dioxide and Water," *Nature Energy* 5, no. 9 (2020): 703–710, https://doi.org/10.1038/s41560-020-0678-6.

59. Q. Wang, T. Hisatomi, Q. Jia, et al., "Scalable Water Splitting on Particulate Photocatalyst Sheets With a Solar-to-Hydrogen Energy Conversion Efficiency Exceeding 1%," *Nature Materials* 15, no. 6 (2016): 611–615, https://doi.org/10.1038/nmat4589.

60. H. Nishiyama, T. Yamada, M. Nakabayashi, et al., "Photocatalytic Solar Hydrogen Production From Water on a 100-m2 Scale," *Nature* 598, no. 7880 (2021): 304–307, https://doi.org/10.1038/s41586-021-03907-3.

61. A. Wang, J. Li, and T. Zhang, "Heterogeneous Single-Atom Catalysis," *Nature Reviews Chemistry* 2, no. 6 (2018): 65–81, https://doi.org/10.1038/s41570-018-0010-1.

62. C. W. Lee, B. H. Lee, S. Park, et al., "Photochemical Tuning of Dynamic Defects for High-Performance Atomically Dispersed Catalysts," *Nature Materials* 23, no. 4 (2024): 552–559, https://doi.org/10.1038/s41563-024-01799-y.

63. Z. Yang, Z. Y. Wu, Z. Lin, et al., "Optically Selective Catalyst Design With Minimized Thermal Emission for Facilitating Photothermal Catalysis," *Nature Communications* 15, no. 1 (2024): 7599, https://doi.org/10.1038/s41467-024-51896-4.

64. G. Perrakis, A. C. Tasolamprou, G. Kenanakis, E. N. Economou, S. Tzortzakis, and M. Kafesaki, "Combined Nano and Micro Structuring for Enhanced Radiative Cooling and Efficiency of Photovoltaic Cells," *Scientific Reports* 11, no. 1 (2021): 11552, https://doi.org/10.1038/s41598-021-91061-1.

65. T. S. Safi and J. N. Munday, "Improving Photovoltaic Performance Through Radiative Cooling in Both Terrestrial and Extraterrestrial Environments," *Optics Express* 23, no. 19 (2015): A1120–A1128, https://doi.org/10.1364/OE.23.0A1120.

66. D. H. Seo, H. R. Kim, J. H. Yun, et al., "Harnessing Outer Space for Improved Electrocaloric Cooling," *Advanced Functional Materials* (2025): 2419891, https://doi.org/10.1002/adfm.202419891.

67. M. Shi, Z. Song, J. Ni, et al., "Dual-Mode Porous Polymeric Films With Coral-Like Hierarchical Structure for All-Day Radiative Cooling and Heating," *ACS Nano* 17, no. 3 (2023): 2029–2038, https://doi.org/10.1021/acsnano.2c07293.

68. Q. Zhang, Y. Lv, Y. Wang, et al., "Temperature-Dependent Dual-Mode Thermal Management Device With Net Zero Energy for Year-Round Energy Saving," *Nature Communications* 13, no. 1 (2022): 4874, https://doi.org/10.1038/s41467-022-32528-1.

69. X. Mei, T. Wang, M. Chen, and L. Wu, "A Self-Adaptive Film for Passive Radiative Cooling and Solar Heating Regulation," *Journal of Materials Chemistry A* 10, no. 20 (2022): 11092–11100, https://doi.org/10.1039/D2TA01291J.

70. C. Guoqi, K. Wang, J. Yang, et al., "Printable Thermochromic Hydrogel-Based Smart Window for All-Weather Building Temperature Regulation in Diverse Climates," *Advanced Materials* 35 (2023): 2211716, https://doi.org/10.1002/adma.202211716.

71. Y. Zhu, Y. Zhou, B. Qin, R. Qin, M. Qiu, and Q. Li, "Night-Time Radiative Warming Using the Atmosphere," *Light: Science & Applications* 12, no. 1 (2023): 268, https://doi.org/10.1038/s41377-023-01315-y.

72. B. Qin, H. Zhu, R. Zhu, M. Zhao, M. Qiu, and Q. Li, "Space-To-Ground Infrared Camouflage With Radiative Heat Dissipation," *Light: Science & Applications* 14, no. 1 (2025): 137, https://doi.org/10.1038/s41377-025-01824-y.

73. M. Zhao, H. Zhu, B. Qin, et al., "High-Temperature Stealth Across Multi-Infrared and Microwave Bands With Efficient Radiative Thermal Management," *Nano-Micro Letters* 17, no. 1 (2025): 199, https://doi.org/10.1007/s40820-025-01712-5.

74. B. Qin, Y. Zhu, Y. Zhou, M. Qiu, and Q. Li, "Whole-Infrared-Band Camouflage With Dual-Band Radiative Heat Dissipation," *Light: Science & Applications* 12, no. 1 (2023): 246, https://doi.org/10.1038/s41377-023-01287-z.

75. X. Cui, Q. Ruan, X. Zhuo, et al., "Photothermal Nanomaterials: A Powerful Light-to-Heat Converter," *Chemical Reviews* 123, no. 11 (2023): 6891–6952, https://doi.org/10.1021/acs.chemrev.3c00159.

76. C. Chen, Y. Kuang, and L. Hu, "Challenges and Opportunities for Solar Evaporation," *Joule* 3, no. 3 (2019): 683–718, https://doi.org/10.1016/j.joule.2018.12.023.

77. L. Zhu, M. Gao, C. K. N. Peh, and G. W. Ho, "Solar-Driven Photothermal Nanostructured Materials Designs and Prerequisites for Evaporation and Catalysis Applications," *Materials Horizons* 5, no. 3 (2018): 323–343, https://doi.org/10.1039/C7MH01064H.

78. A. Amri, Z. T. Jiang, T. Pryor, C. Y. Yin, and S. Djordjevic, "Developments in the Synthesis of Flat Plate Solar Selective Absorber Materials via Sol–Gel Methods: A Review," *Renewable and Sustainable Energy Reviews* 36 (2014): 316–328, https://doi.org/10.1016/j.rser.2014.04.062.

79. J. Zeng, D. Goldfeld, and Y. Xia, "A Plasmon-Assisted Optofluidic (PAOF) System for Measuring the Photothermal Conversion Efficiencies of Gold Nanostructures and Controlling an Electrical Switch," *Angewandte Chemie International Edition* 52, no. 15 (2013): 4169–4173, https://doi.org/10.1002/anie.201210359.

80. L. Xiao, X. Chen, X. Yang, J. Sun, and J. Geng, "Recent Advances in Polymer-Based Photothermal Materials for Biological Applications," *ACS Applied Polymer Materials* 2, no. 10 (2020): 4273–4288, https://doi.org/10.1021/acsapm.0c00711.

81. M. J. Yoo, K. R. Pyun, Y. Jung, M. Lee, J. Lee, and S. H. Ko, "Switchable Radiative Cooling and Solar Heating for Sustainable Thermal Management," *Nanophotonics* 13, no. 5 (2024): 543–561, https://doi.org/10.1515/nanoph-2023-0627.

82. T. Wang, Y. Wu, L. Shi, X. Hu, M. Chen, and L. Wu, "A Structural Polymer for Highly Efficient All-Day Passive Radiative Cooling," *Nature Communications* 12, no. 1 (2021): 365, https://doi.org/10.1038/s41467-020-20646-7.

83. F. Xie, W. Jin, J. R. Nolen, et al., "Subambient Daytime Radiative Cooling of Vertical Surfaces," *Science* 386, no. 6723 (2024): 788–794, https://doi.org/10.1126/science.adn2524.

84. A. Azens and C. Granqvist, "Electrochromic Smart Windows: Energy Efficiency and Device Aspects," *Journal of Solid State Electrochemistry* 7, no. 2 (2003): 64–68, https://doi.org/10.1007/s10008-002-0313-4.

85. P. Cheng, D. Wang, and P. Schaaf, "A Review on Photothermal Conversion of Solar Energy With Nanomaterials and Nanostructures: From Fundamentals to Applications," *Advanced Sustainable Systems* 6, no. 9 (2022): 2200115, https://doi.org/10.1002/adsu.202200115.

86. Y. Dong, X. Zhang, L. Chen, et al., "Progress in Passive Daytime Radiative Cooling: A Review From Optical Mechanism, Performance Test, and Application," *Renewable and Sustainable Energy Reviews* 188 (2023): 113801, https://doi.org/10.1016/j.rser.2023.113801.

87. J. Liang, J. Wu, J. Guo, et al., "Radiative Cooling for Passive Thermal Management Towards Sustainable Carbon Neutrality," *National Science Review* 10, no. 1 (2023): nwac208, https://doi.org/10.1093/nsr/nwac208.

88. W. Wang, Z. Zhao, Q. Zou, B. Hong, W. Zhang, and G. P. Wang, "Self-Adaptive Radiative Cooling and Solar Heating Based on a Compound Metasurface," *Journal of Materials Chemistry C* 8, no. 9 (2020): 3192–3199, https://doi.org/10.1039/C9TC05634C.

89. Y. Zhai, Y. Ma, S. N. David, et al., "Scalable-Manufactured Randomized Glass-Polymer Hybrid Metamaterial for Daytime Radiative Cooling," *Science* 355, no. 6329 (2017): 1062–1066, https://doi.org/10.1126/science.aai7899.

90. Y. Li, Y. Shi, H. Wang, et al., "Recent Advances in Carbon-Based Materials for Solar-Driven Interfacial Photothermal Conversion Water Evaporation: Assemblies, Structures, Applications, and Prospective," *Carbon Energy* 5, no. 11 (2023): e331, https://doi.org/10.1002/cey2.331.

91. L. Jauffred, A. Samadi, H. Klingberg, P. Bendix, and L. Oddershede, "Plasmonic Heating of Nanostructures," *Chemical Reviews* 119 (2019): 8087–8130, https://doi.org/10.1021/acs.chemrev.8b00738.

92. M. Kim, J. H. Lee, and J. M. Nam, "Plasmonic Photothermal Nanoparticles for Biomedical Applications," *Advancement of Science* 6, no. 17 (2019): 1900471, https://doi.org/10.1002/advs.201900471.

93. J. H. Han, D. Kim, J. Kim, G. Kim, P. Fischer, and H. H. Jeong, "Plasmonic Nanostructure Engineering With Shadow Growth,"

Advanced Materials 35, no. 34 (2023): 2107917, https://doi.org/10.1002/adma.202107917.

94. X. Huang, W. Zhang, G. Guan, G. Song, R. Zou, and J. Hu, "Design and Functionalization of the NIR-Responsive Photothermal Semiconductor Nanomaterials for Cancer Theranostics," *Accounts of Chemical Research* 50 (2017): 2529–2538, https://doi.org/10.1021/acs.accounts.7b00294.

95. I. Kriegel, F. Scotognella, and L. Manna, "Plasmonic Doped Semiconductor Nanocrystals: Properties, Fabrication, Applications and Perspectives," *Physics Reports* 674 (2017): 1–52, https://doi.org/10.1016/j.physrep.2017.01.003.

96. N. Panwar, A. Soehartono, K. K. Chan, et al., "Nanocarbons for Biology and Medicine: Sensing, Imaging, and Drug Delivery," *Chemical Reviews* 119 (2019): 9559–9656, https://doi.org/10.1021/acs.chemrev.9b00099.

97. B. Wang, H. Song, X. Qu, J. Chang, B. Yang, and S. Lu, "Carbon Dots as a New Class of Nanomedicines: Opportunities and Challenges," *Coordination Chemistry Reviews* 442 (2021): 214010, https://doi.org/10.1016/j.ccr.2021.214010.

98. J. Du, N. Xu, J. Fan, W. Sun, and X. Peng, "Carbon Dots for In Vivo Bioimaging and Theranostics," *Small* 15, no. 32 (2019): 1805087, https://doi.org/10.1002/smll.201805087.

99. H. S. Jung, P. Verwilst, A. Sharma, J. Shin, J. L. Sessler, and J. S. Kim, "Organic Molecule-Based Photothermal Agents: An Expanding Photothermal Therapy Universe," *Chemical Society Reviews* 47, no. 7 (2018): 2280–2297, https://doi.org/10.1039/C7CS00522A.

100. M. Lee, G. Kim, Y. Jung, et al., "Photonic Structures in Radiative Cooling," *Light: Science & Applications* 12, no. 1 (2023): 134, https://doi.org/10.1038/s41377-023-01119-0.

101. J. Jaramillo-Fernandez, G. L. Whitworth, J. A. Pariente, et al., "A Self-Assembled 2D Thermofunctional Material for Radiative Cooling," *Small* 15, no. 52 (2019): 1905290, https://doi.org/10.1002/smll.201905290.

102. R. Liu, S. Wang, Z. Zhou, et al., "Materials in Radiative Cooling Technologies," *Advanced Materials* 37, no. 2 (2025): 2401577, https://doi.org/10.1002/adma.202401577.

103. J. H. Han, J. Kim, G. Kim, et al., "Dichroic Engineering From Invisible to Full Colors Using Plasmonics," *Advanced Functional Materials* 34, no. 28 (2024): 2314434, https://doi.org/10.1002/adfm.202314434.

104. G. Kim, D. Kim, S. Ko, et al., "Programmable Directional Color Dynamics Using Plasmonics," *Microsystems & Nanoengineering* 10, no. 1 (2024): 22, https://doi.org/10.1038/s41378-023-00635-8.

105. S. Linic, U. Aslam, C. Boerigter, and M. Morabito, "Erratum: Photochemical Transformations on Plasmonic Metal Nanoparticles," *Nature Materials* 14 (2015): 567–576, https://doi.org/10.1038/nmat4281.

106. G. Baffou and R. Quidant, "Thermo-Plasmonics: Using Metallic Nanostructures as Nano-Sources of Heat," *Laser & Photonics Reviews* 7, no. 2 (2013): 171–187, https://doi.org/10.1002/lpor.201200003.

107. G. Baffou, I. Bordacchini, A. Baldi, and R. Quidant, "Simple Experimental Procedures to Distinguish Photothermal From Hot-Carrier Processes in Plasmonics," *Light: Science & Applications* 9, no. 1 (2020): 108, https://doi.org/10.1038/s41377-020-00345-0.

108. A. Lalisse, G. Tessier, J. Plain, and G. Baffou, "Quantifying the Efficiency of Plasmonic Materials for Near-Field Enhancement and Photothermal Conversion," *Journal of Physical Chemistry C* 119, no. 45 (2015): 25518–25528, https://doi.org/10.1021/acs.jpcc.5b09294.

109. G. Kim, D. Kim, J. Lee, et al., "Quasi-Ordered Plasmonic Metasurfaces With Unclonable Stochastic Scattering for Secure Authentication," *Nature Communications* 16 (2025): 6269.

110. J. Chen, Z. Ye, F. Yang, and Y. Yin, "Plasmonic Nanostructures for Photothermal Conversion," *Small Science* 1, no. 2 (2021): 2000055, https://doi.org/10.1002/smsc.202000055.

111. T. T. D. Pham, L. M. T. Phan, S. Cho, and J. Park, "Enhancement Approaches for Photothermal Conversion of Donor–Acceptor Conjugated Polymer for Photothermal Therapy: A Review," *Science and Technology of Advanced Materials* 23, no. 1 (2022): 707–734, https://doi.org/10.1080/14686996.2022.2134976.

112. W. W. Gärtner, "Photothermal Effect in Semiconductors," *Physics Review* 122, no. 2 (1961): 419–424, https://doi.org/10.1103/PhysRev.122.419.

113. X. Chen, L. Liu, P. Y. Yu, and S. S. Mao, "Increasing Solar Absorption for Photocatalysis With Black Hydrogenated Titanium Dioxide Nanocrystals," *Science* 331, no. 6018 (2011): 746–750, https://doi.org/10.1126/science.1200448.

114. J. M. Luther, P. K. Jain, T. Ewers, and A. P. Alivisatos, "Localized Surface Plasmon Resonances Arising From Free Carriers in Doped Quantum Dots," *Nature Materials* 10, no. 5 (2011): 361–366, https://doi.org/10.1038/nmat3004.

115. D. Xu, Z. Li, L. Li, and J. Wang, "Insights Into the Photothermal Conversion of 2D MXene Nanomaterials: Synthesis, Mechanism, and Applications," *Advanced Functional Materials* 30, no. 47 (2020): 2000712, https://doi.org/10.1002/adfm.202000712.

116. W. He, L. Zhou, M. Wang, Y. Cao, X. Chen, and X. Hou, "Structure Development of Carbon-Based Solar-Driven Water Evaporation Systems," *Scientific Bulletin* 66, no. 14 (2021): 1472–1483, https://doi.org/10.1016/j.scib.2021.02.014.

117. Y. Wang, H. M. Meng, G. Song, Z. Li, and X. B. Zhang, "Conjugated-Polymer-Based Nanomaterials for Photothermal Therapy," *ACS Applied Polymer Materials* 2, no. 10 (2020): 4258–4272, https://doi.org/10.1021/acsapm.0c00680.

118. C. Yu, L. Xu, Y. Zhang, P. S. Timashev, Y. Huang, and X. J. Liang, "Polymer-Based Nanomaterials for Noninvasive Cancer Photothermal Therapy," *ACS Applied Polymer Materials* 2, no. 10 (2020): 4289–4305, https://doi.org/10.1021/acsapm.0c00704.

119. A. R. Gentle and G. B. Smith, "Radiative Heat Pumping From the Earth Using Surface Phonon Resonant Nanoparticles," *Nano Letters* 10, no. 2 (2010): 373–379, https://doi.org/10.1021/nl903271d.

120. L. Tang, J. DeSutter, and M. Francoeur, "Near-Field Radiative Heat Transfer Between Dissimilar Materials Mediated by Coupled Surface Phonon- and Plasmon-Polaritons," *ACS Photonics* 7, no. 5 (2020): 1304–1311, https://doi.org/10.1021/acsphotonics.0c00404.

121. A. K. Goyal, H. S. Dutta, and S. Pal, "Design and Analysis of Photonic Crystal Micro-Cavity Based Optical Sensor Platform," *AIP Conference Proceedings* 1724, no. 1 (2016): 20005, https://doi.org/10.1063/1.4945125.

122. L. Zhu, A. Raman, and S. Fan, "Color-Preserving Daytime Radiative Cooling," *Applied Physics Letters* 103 (2013): 223902, https://doi.org/10.1063/1.4835995.

123. Y. Zhang, T. Wang, X. Mei, H. Tu, M. Chen, and L. Wu, "Bioinspired Design of a Binary Synergistic Photonic Structure for Daytime Radiative Cooling," *ACS Photonics* 11, no. 5 (2024): 1960–1968, https://doi.org/10.1021/acsphotonics.4c00057.

124. S. So, Y. Yang, S. Son, et al., "Highly Suppressed Solar Absorption in a Daytime Radiative Cooler Designed by Genetic Algorithm," *Nanophotonics* 11, no. 9 (2022): 2107–2115, https://doi.org/10.1515/nanoph-2021-0436.

125. E. Rephaeli, A. Raman, and S. Fan, "Ultrabroadband Photonic Structures to Achieve High-Performance Daytime Radiative Cooling," *Nano Letters* 13, no. 4 (2013): 1457–1461, https://doi.org/10.1021/nl4004283.

126. M. Hossain, B. Jia, and M. Gu, "Metamaterials: A Metamaterial Emitter for Highly Efficient Radiative Cooling," *Advanced Optical Materials* 3 (2015): 980, https://doi.org/10.1002/adom.201570046.

127. C. Ji, K. T. Lee, T. Xu, J. Zhou, H. J. Park, and L. Guo, "Engineering Light at the Nanoscale: Structural Color Filters and Broadband Perfect

Absorbers," *Advanced Optical Materials* 5 (2017): 1700368, https://doi.org/10.1002/adom.201700368.

128. A. Kong, B. Cai, P. Shi, and X. Yuan, "Ultra-Broadband All-Dielectric Metamaterial Thermal Emitter for Passive Radiative Cooling," *Optics Express* 27, no. 21 (2019): 30102–30115, https://doi.org/10.1364/OE.27.030102.

129. H. Yuan, C. Yang, X. Zheng, et al., "Effective, Angle-Independent Radiative Cooler Based on One-Dimensional Photonic Crystal," *Optics Express* 26 (2018): 27885–27893, https://doi.org/10.1364/OE.26.027885.

130. W. X. Tang, H. C. Zhang, H. F. Ma, W. X. Jiang, and T. J. Cui, "Concept, Theory, Design, and Applications of Spoof Surface Plasmon Polaritons at Microwave Frequencies," *Advanced Optical Materials* 7, no. 1 (2019): 1800421, https://doi.org/10.1002/adom.201800421.

131. S. Y. Heo, G. J. Lee, D. H. Kim, et al., "A Janus Emitter for Passive Heat Release From Enclosures," *Science Advances* 6, no. 36 (2025): eabb1906, https://doi.org/10.1126/sciadv.abb1906.

132. K. Amano, M. Matsuoka, T. Nakamura, et al., "Reassigning CI Chondrite Parent Bodies Based on Reflectance Spectroscopy of Samples From Carbonaceous Asteroid Ryugu and Meteorites," *Science Advances* 9, no. 49 (2025): eadi3789, https://doi.org/10.1126/sciadv.adi3789.

133. S. Xue, G. Huang, Q. Chen, X. Wang, J. Fan, and D. Shou, "Personal Thermal Management by Radiative Cooling and Heating," *Nano-Micro Letters* 16, no. 1 (2024): 153, https://doi.org/10.1007/s40820-024-01360-1.

134. J. Zhu, Z. An, A. Zhang, et al., "Anisotropic Porous Designed Polymer Coatings for High-Performance Passive All-Day Radiative Cooling," *iScience* 25, no. 4 (2022): 104126, https://doi.org/10.1016/j.isci.2022.104126.

135. M. A. A. Beg and H. C. Clark, "Chemistry of the Trifluoromethyl Group: Part V. Infrared Spectra of Some Phosphorus Compounds Containing CF3," *Canadian Journal of Chemistry* 40, no. 3 (1962): 393–398, https://doi.org/10.1139/v62-063.

136. Z. Zhou, X. Wang, Y. Ma, B. Hu, and J. Zhou, "Transparent Polymer Coatings for Energy-Efficient Daytime Window Cooling," *Cell Reports Physical Science* 1, no. 11 (2020): 100231, https://doi.org/10.1016/j.xcrp.2020.100231.

137. O. Teresa and C. K. Choi, "Comparison Between SiOC Thin Film by Plasma Enhance Chemical Vapor Deposition and SiO_2 Thin Film by Fourier Transform Infrared Spectroscopy," *Journal of the Korean Physical Society* 56 (2010): 1150–1155, https://doi.org/10.3938/jkps.56.1150.

138. H. Park, B. S. Joo, G. Kang, H. Ko, and J. H. Kim, "A Hierarchically Engineered Polymer Composite With a Dual-Scatter Structure for Enhanced Passive Radiative Cooling," *Journal of Materials Chemistry A* 13, no. 7 (2025): 4870–4880, https://doi.org/10.1039/D4TA07793H.

139. M. M. Hossain and M. Gu, "Radiative Cooling: Principles, Progress, and Potentials," *Advancement of Science* 3, no. 7 (2016): 1500360, https://doi.org/10.1002/advs.201500360.

140. S. Vall and A. Castell, "Radiative Cooling as Low-Grade Energy Source: A Literature Review," *Renewable and Sustainable Energy Reviews* 77 (2017): 803–820, https://doi.org/10.1016/j.rser.2017.04.010.

141. K. Zhang, D. Zhao, X. Yin, R. Yang, and G. Tan, "Energy Saving and Economic Analysis of a New Hybrid Radiative Cooling System for Single-Family Houses in the USA," *Applied Energy* 224 (2018): 371–381, https://doi.org/10.1016/j.apenergy.2018.04.115.

142. M. Hanif, T. M. I. Mahlia, A. Zare, T. J. Saksahdan, and H. S. C. Metselaar, "Potential Energy Savings by Radiative Cooling System for a Building in Tropical Climate," *Renewable and Sustainable Energy Reviews* 32 (2014): 642–650, https://doi.org/10.1016/j.rser.2014.01.053.

143. S. Suhendri, M. Hu, Y. Dan, Y. Su, B. Zhao, and S. Riffat, "Building Energy-Saving Potential of a Dual-Functional Solar Heating and Radiative Cooling System," *Energy and Buildings* 303 (2024): 113764, https://doi.org/10.1016/j.enbuild.2023.113764.

144. X. Yue, T. Zhang, D. Yang, F. Qiu, G. Wei, and H. Zhou, "Multifunctional Janus Fibrous Hybrid Membranes With Sandwich Structure for On-Demand Personal Thermal Management," *Nano Energy* 63 (2019): 103808, https://doi.org/10.1016/j.nanoen.2019.06.004.

145. S. Wang, T. Jiang, Y. Meng, R. Yang, G. Tan, and Y. Long, "Scalable Thermochromic Smart Windows With Passive Radiative Cooling Regulation," *Science* 374, no. 6574 (2021): 1501–1504, https://doi.org/10.1126/science.abg0291.

146. C. Sui, J. Pu, T. H. Chen, et al., "Dynamic Electrochromism for All-Season Radiative Thermoregulation," *Nature Sustainability* 6, no. 4 (2023): 428–437, https://doi.org/10.1038/s41893-022-01023-2.

147. M. Yang, H. Zhong, T. Li, B. Wu, Z. Wang, and D. Sun, "Phase Change Material Enhanced Radiative Cooler for Temperature-Adaptive Thermal Regulation," *ACS Nano* 17, no. 2 (2023): 1693–1700, https://doi.org/10.1021/acsnano.2c11916.

148. C. Kuang, S. Chen, M. Liao, et al., "Electrically Tunable Infrared Optics Enabled by Flexible Ion-Permeable Conducting Polymer-Cellulose Paper," *npj Flexible Electronics* 8, no. 1 (2024): 55, https://doi.org/10.1038/s41528-024-00339-7.

149. J. H. Ko, Y. J. Yoo, Y. Lee, H. H. Jeong, and Y. M. Song, "A Review of Tunable Photonics: Optically Active Materials and Applications From Visible to Terahertz," *iScience* 25, no. 8 (2022): 104727, https://doi.org/10.1016/j.isci.2022.104727.

150. P. Prabhathan, K. V. Sreekanth, J. Teng, et al., "Roadmap for Phase Change Materials in Photonics and Beyond," *iScience* 26, no. 10 (2023): 107946, https://doi.org/10.1016/j.isci.2023.107946.

151. C. Jung, S. J. Kim, J. Jang, et al., "Disordered-Nanoparticle–Based Etalon for Ultrafast Humidity-Responsive Colorimetric Sensors and Anti-Counterfeiting Displays," *Science Advances* 8, no. 10 (2025): eabm8598, https://doi.org/10.1126/sciadv.abm8598.

152. Y. J. Yoo, W. G. Kim, J. H. Ko, et al., "Large-Area Virus Coated Ultrathin Colorimetric Sensors With a Highly Lossy Resonant Promoter for Enhanced Chromaticity," *Advanced Science* 7, no. 18 (2020): 2000978, https://doi.org/10.1002/advs.202000978.

153. B. Ko, J. Kim, Y. Yang, et al., "Humidity-Responsive RGB-Pixels via Swelling of 3D Nanoimprinted Polyvinyl Alcohol," *Advancement of Science* 10, no. 2 (2023): 2204469, https://doi.org/10.1002/advs.202204469.

154. Y. J. Yoo, J. H. Ko, W. G. Kim, et al., "Dual-Mode Colorimetric Sensor Based on Ultrathin Resonating Facilitator Capable of Nanometer-Thick Virus Detection for Environment Monitoring," *ACS Applied Nano Materials* 3, no. 7 (2020): 6636–6644, https://doi.org/10.1021/acsanm.0c01067.

155. H. J. Nam, J. H. Ko, H. E. Jeong, et al., "Ultrafast, Fano Resonant Colorimetric Sensor With High Chromaticity Beyond Standard RGB," *Optica* 11, no. 10 (2024): 1425–1436, https://doi.org/10.1364/OPTICA.532433.

156. S. Zhang, Z. Liu, W. Zhang, et al., "Multi-Bioinspired Flexible Thermal Emitters for All-Day Radiative Cooling and Wearable Self-Powered Thermoelectric Generation," *Nano Energy* 123 (2024): 109393, https://doi.org/10.1016/j.nanoen.2024.109393.

157. J. H. Ko, J. E. Yeo, H. E. Jeong, et al., "Switchable and Conspicuous Retroreflective Sensors Inspired by the Wing Scale of an Emerald Swallowtail," *Biosensors & Bioelectronics* 260 (2024): 116445, https://doi.org/10.1016/j.bios.2024.116445.

158. J. H. Ko, D. H. Kim, S. H. Hong, S. K. Kim, and Y. M. Song, "Polarization-Driven Thermal Emission Regulator Based on Self-Aligned GST Nanocolumns," *iScience* 26, no. 1 (2023): 105780, https://doi.org/10.1016/j.isci.2022.105780.

159. J. H. Ko, D. H. Seo, H. H. Jeong, S. Kim, and Y. M. Song, "Sub-1-Volt Electrically Programmable Optical Modulator Based on Active Tamm

Plasmon," *Advanced Materials* 36, no. 15 (2024): 2310556, https://doi.org/10.1002/adma.202310556.

160. J. H. Ko, J. E. Yeo, H. E. Jeong, et al., "Electrochromic Nanopixels With Optical Duality for Optical Encryption Applications," *Nanophotonics* 13, no. 7 (2024): 1119–1129, https://doi.org/10.1515/nanoph-2023-0737.

161. J. H. Ko, D. H. Seo, S. Y. Kim, Y. Lee, K. Park, and Y. M. Song, "Optically Readable Synaptic Modulators Based on Tamm Plasmon for Adaptive Multispectral Image Processing," *iScience* 28, no. 2 (2025): 111800, https://doi.org/10.1016/j.isci.2025.111800.

162. Y. Ding, Z. Mei, X. Wu, et al., "Integrated Multispectral Modulator With Efficient Radiative Cooling for Innovative Thermal Camouflage," *Advanced Functional Materials* (2025): 2500122, https://doi.org/10.1002/adfm.202500122.

163. J. Tang, H. Ni, R. L. Peng, N. Wang, and L. Zuo, "A Review on Energy Conversion Using Hybrid Photovoltaic and Thermoelectric Systems," *Journal of Power Sources* 562 (2023): 232785, https://doi.org/10.1016/j.jpowsour.2023.232785.

164. B. Zhao, M. Hu, X. Ao, Q. Xuan, Z. Song, and G. Pei, "Is It Possible for a Photovoltaic-Thermoelectric Device to Generate Electricity at Night?," *Solar Energy Materials & Solar Cells* 228 (2021): 111136, https://doi.org/10.1016/j.solmat.2021.111136.

165. M. Liao, D. Banerjee, T. Hallberg, et al., "Cellulose-Based Radiative Cooling and Solar Heating Powers Ionic Thermoelectrics," *Advanced Science* 10, no. 8 (2023): 2206510, https://doi.org/10.1002/advs.202206510.

166. W. B. Han, S. Y. Heo, D. Kim, et al., "Zebra-Inspired Stretchable, Biodegradable Radiation Modulator for All-Day Sustainable Energy Harvesters," *Science Advances* 9, no. 5 (2025): eadf5883, https://doi.org/10.1126/sciadv.adf5883.

167. J. Z. Liu, W. Jiang, S. Zhuo, et al., "Large-Area Radiation-Modulated Thermoelectric Fabrics for High-Performance Thermal Management and Electricity Generation," *Science Advances* 11, no. 1 (2025): eadr2158, https://doi.org/10.1126/sciadv.adr2158.

168. Y. Liu, S. Hou, X. Wang, et al., "Passive Radiative Cooling Enables Improved Performance in Wearable Thermoelectric Generators," *Small* 18, no. 10 (2022): 2106875, https://doi.org/10.1002/smll.202106875.

169. S. Zhang, Z. Wu, Z. Liu, et al., "Power Generation on Chips: Harvesting Energy From the Sun and Cold Space," *Advanced Materials Technologies* 7, no. 12 (2022): 2200478, https://doi.org/10.1002/admt.202200478.

170. K. Gao, J. Yang, H. Shen, Y. Liu, Y. Li, and M. Zhang, "Uninterrupted Self-Generation Thermoelectric Power Device Based on the Radiative Cooling Emitter and Solar Selective Absorber," *Solar RRL* 6, no. 2 (2022): 2100975, https://doi.org/10.1002/solr.202100975.

171. C. H. Wang, H. Chen, Z. Y. Jiang, and X. X. Zhang, "Design and Experimental Validation of an All-Day Passive Thermoelectric System via Radiative Cooling and Greenhouse Effects," *Energy* 263 (2023): 125735, https://doi.org/10.1016/j.energy.2022.125735.

172. J. Li, Y. Fu, J. Zhou, et al., "Ultrathin, Soft, Radiative Cooling Interfaces for Advanced Thermal Management in Skin Electronics," *Science Advances* 9, no. 14 (2025): eadg1837, https://doi.org/10.1126/sciadv.adg1837.

173. P. Tao, G. Ni, C. Song, et al., "Solar-Driven Interfacial Evaporation," *Nature Energy* 3, no. 12 (2018): 1031–1041, https://doi.org/10.1038/s41560-018-0260-7.

174. M. C and A. Yadav, "Water Desalination System Using Solar Heat: A Review," *Renewable and Sustainable Energy Reviews* 67 (2017): 1308–1330, https://doi.org/10.1016/j.rser.2016.08.058.

175. O. Neumann, C. Feronti, A. D. Neumann, et al., "Compact Solar Autoclave Based on Steam Generation Using Broadband Light-Harvesting Nanoparticles," *Proceedings of the National Academy of Sciences* 110, no. 29 (2013): 11677–11681, https://doi.org/10.1073/pnas.1310131110.

176. O. K. Varghese, M. Paulose, T. J. LaTempa, and C. A. Grimes, "High-Rate Solar Photocatalytic Conversion of CO_2 and Water Vapor to Hydrocarbon Fuels," *Nano Letters* 9, no. 2 (2009): 731–737, https://doi.org/10.1021/nl803258p.

177. P. Yang, K. Liu, Q. Chen, et al., "Solar-Driven Simultaneous Steam Production and Electricity Generation From Salinity," *Energy & Environmental Science* 10, no. 9 (2017): 1923–1927, https://doi.org/10.1039/C7EE01804E.

178. X. Li, J. Zhang, Y. Liu, et al., "Fish-Inspired Dynamic Charging for Ultrafast Self-Protective Solar-Thermal Energy Storage," *Science Advances* 10, no. 49 (2025): eadr8445, https://doi.org/10.1126/sciadv.adr8445.

179. L. Zhang, X. Li, Y. Zhong, et al., "Highly Efficient and Salt Rejecting Solar Evaporation via a Wick-Free Confined Water Layer," *Nature Communications* 13, no. 1 (2022): 849, https://doi.org/10.1038/s41467-022-28457-8.

180. X. Zhao, H. Zhang, K. Y. Chan, X. Huang, Y. Yang, and X. Shen, "Tree-Inspired Structurally Graded Aerogel With Synergistic Water, Salt, and Thermal Transport for High-Salinity Solar-Powered Evaporation," *Nano-Micro Letters* 16, no. 1 (2024): 222, https://doi.org/10.1007/s40820-024-01448-8.

181. L. Zou, Y. Zou, B. Wu, H. Liu, X. Li, and X. Wu, "Ultra-Broadband and Wide-Angle Solar Absorber With Hierarchical Nanohole Design Based on MXene," *International Journal of Thermal Sciences* 197 (2024): 108764, https://doi.org/10.1016/j.ijthermalsci.2023.108764.

182. L. Zhou, Y. Tan, D. Ji, et al., "Self-Assembly of Highly Efficient, Broadband Plasmonic Absorbers for Solar Steam Generation," *Science Advances* 2, no. 4 (2025): e1501227, https://doi.org/10.1126/sciadv.1501227.

183. X. Chen, S. Liu, N. Yang, R. Yu, and D. Wang, "Hierarchical Structure Regulation for Sequential Steps in Solar Vapor Generation," *EcoMat* 5, no. 7 (2023): e12348, https://doi.org/10.1002/eom2.12348.

184. L. Zhang, Z. Xu, L. Zhao, et al., "Passive, High-Efficiency Thermally-Localized Solar Desalination," *Energy & Environmental Science* 14, no. 4 (2021): 1771–1793, https://doi.org/10.1039/D0EE03991H.

185. Y. Xia, Q. Hou, H. Jubaer, et al., "Spatially Isolating Salt Crystallisation From Water Evaporation for Continuous Solar Steam Generation and Salt Harvesting," *Energy & Environmental Science* 12, no. 6 (2019): 1840–1847, https://doi.org/10.1039/C9EE00692C.

186. T. A. Cooper, S. H. Zandavi, G. W. Ni, et al., "Contactless Steam Generation and Superheating Under One Sun Illumination," *Nature Communications* 9, no. 1 (2018): 5086, https://doi.org/10.1038/s41467-018-07494-2.

187. Z. Lei, S. Zhu, X. Sun, et al., "A Multiscale Porous 3D-Fabric Evaporator With Vertically Aligned Yarns Enables Ultra-Efficient and Continuous Water Desalination," *Advanced Functional Materials* 32, no. 40 (2022): 2205790, https://doi.org/10.1002/adfm.202205790.

188. W. Ma, T. Lu, W. Cao, R. Xiong, and C. Huang, "Bioinspired Nanofibrous Aerogel With Vertically Aligned Channels for Efficient Water Purification and Salt-Rejecting Solar Desalination," *Advanced Functional Materials* 33, no. 23 (2023): 2214157, https://doi.org/10.1002/adfm.202214157.

189. L. Wu, Z. Dong, Z. Cai, et al., "Highly Efficient Three-Dimensional Solar Evaporator for High Salinity Desalination by Localized Crystallization," *Nature Communications* 11 (2020): 521, https://doi.org/10.1038/s41467-020-14366-1.

190. X. Dong, Y. Si, C. Chen, B. Ding, and H. Deng, "Reed Leaves Inspired Silica Nanofibrous Aerogels With Parallel-Arranged Vessels for Salt-Resistant Solar Desalination," *ACS Nano* 15, no. 7 (2021): 12256–12266, https://doi.org/10.1021/acsnano.1c04035.

191. M. Gao, T. Zhang, and G. W. Ho, “Advances of Photothermal Chemistry in Photocatalysis, Thermocatalysis, and Synergetic Photothermocatalysis for Solar-to-Fuel Generation,” *Nano Research* 15, no. 12 (2022): 9985–10005, https://doi.org/10.1007/s12274-022-4795-3.

192. W. H. Lee, C. W. Lee, G. D. Cha, et al., “Floatable Photocatalytic Hydrogel Nanocomposites for Large-Scale Solar Hydrogen Production,” *Nature Nanotechnology* 18, no. 7 (2023): 754–762, https://doi.org/10.1038/s41565-023-01385-4.

193. Y. Yao, B. Li, X. Gao, et al., “Highly Efficient Solar-Driven Dry Reforming of Methane on a rh/LaNiO3 Catalyst Through a Light-Induced Metal-To-Metal Charge Transfer Process,” *Advanced Materials* 35, no. 39 (2023): 2303654, https://doi.org/10.1002/adma.202303654.

194. L. Zhou, J. M. P. Martirez, J. Finzel, et al., “Light-Driven Methane Dry Reforming With Single Atomic Site Antenna-Reactor Plasmonic Photocatalysts,” *Nature Energy* 5, no. 1 (2020): 61–70, https://doi.org/10.1038/s41560-019-0517-9.

195. M. Cai, Z. Wu, Z. Li, et al., “Greenhouse-Inspired Supra-Photothermal CO_2 Catalysis,” *Nature Energy* 6, no. 8 (2021): 807–814, https://doi.org/10.1038/s41560-021-00867-w.

196. H. Song, S. Luo, H. Huang, B. Deng, and J. Ye, “Solar-Driven Hydrogen Production: Recent Advances, Challenges, and Future Perspectives,” *ACS Energy Letters* 7, no. 3 (2022): 1043–1065, https://doi.org/10.1021/acsenergylett.1c02591.

197. K. K. Ghuman, L. B. Hoch, P. Szymanski, et al., “Photoexcited Surface Frustrated Lewis Pairs for Heterogeneous Photocatalytic CO_2 Reduction,” *Journal of the American Chemical Society* 138, no. 4 (2016): 1206–1214, https://doi.org/10.1021/jacs.5b10179.

198. K. Yoshikawa, H. Kawasaki, W. Yoshida, et al., “Silicon Heterojunction Solar Cell With Interdigitated Back Contacts for a Photoconversion Efficiency Over 26%,” *Nature Energy* 2, no. 5 (2017): 17032, https://doi.org/10.1038/nenergy.2017.32.

199. L. Zhu, A. Raman, K. X. Wang, M. A. Anoma, and S. Fan, “Radiative Cooling of Solar Cells,” *Optica* 1, no. 1 (2014): 32–38, https://doi.org/10.1364/OPTICA.1.000032.

200. S. Y. Heo, D. H. Kim, Y. M. Song, and G. J. Lee, “Determining the Effectiveness of Radiative Cooler-Integrated Solar Cells,” *Advanced Energy Materials* 12, no. 10 (2022): 2103258, https://doi.org/10.1002/aenm.202103258.

201. Y. Lu, Z. Chen, L. Ai, et al., “A Universal Route to Realize Radiative Cooling and Light Management in Photovoltaic Modules,” *Solar RRL* 1, no. 10 (2017): 1700084, https://doi.org/10.1002/solr.201700084.

202. Z. Wang, D. Kortge, J. Zhu, et al., “Lightweight, Passive Radiative Cooling to Enhance Concentrating Photovoltaics,” *Joule* 4, no. 12 (2020): 2702–2717, https://doi.org/10.1016/j.joule.2020.10.004.

203. Z. Zhou, Z. Wang, and P. Bermel, “Radiative Cooling for Low-Bandgap Photovoltaics Under Concentrated Sunlight,” *Optics Express* 27, no. 8 (2019): A404–A418, https://doi.org/10.1364/OE.27.00A404.

204. D. Bredemeier, D. Walter, S. Herlufsen, and J. Schmidt, “Lifetime Degradation and Regeneration in Multicrystalline Silicon Under Illumination at Elevated Temperature,” *AIP Advances* 6, no. 3 (2016): 35119, https://doi.org/10.1063/1.4944839.

205. D. C. Jordan and S. R. Kurtz, “Photovoltaic Degradation Rates—An Analytical Review,” *Progress in Photovoltaics: Research and Applications* 21, no. 1 (2013): 12–29, https://doi.org/10.1002/pip.1182.

206. M. J. Huang, P. C. Eames, and B. Norton, “Thermal Regulation of Building-Integrated Photovoltaics Using Phase Change Materials,” *International Journal of Heat and Mass Transfer* 47, no. 12 (2004): 2715–2733, https://doi.org/10.1016/j.ijheatmasstransfer.2003.11.015.

207. Z. Xu, H. Luo, H. Zhu, et al., “Nonvolatile Optically Reconfigurable Radiative Metasurface With Visible Tunability for Anticounterfeiting,” *Nano Letters* 21, no. 12 (2021): 5269–5276, https://doi.org/10.1021/acs.nanolett.1c01396.

208. J. R. Nolen, A. C. Overvig, M. Cotrufo, and A. Alù, “Local Control of Polarization and Geometric Phase in Thermal Metasurfaces,” *Nature Nanotechnology* 19, no. 11 (2024): 1627–1634, https://doi.org/10.1038/s41565-024-01763-6.

209. J. Yu, R. Qin, Y. Ying, M. Qiu, and Q. Li, “Asymmetric Directional Control of Thermal Emission,” *Advanced Materials* 35, no. 45 (2023): 2302478, https://doi.org/10.1002/adma.202302478.

210. H. R. Kim, W. B. Han, S.-Y. Heo, et al., “Bio-Inspired Strategy for Radiation-Based Thermal Management and Utilization,” *Advanced Science* (2025): e02851.